

**PROTEOMIC ANALYSIS OF TURNIP CRINKLE
VIRUS-INFECTED TOBACCO USING 2-D GEL
ELECTROPHORESIS**

XIE JUNTAO

(B.Sc.)

**A THESIS SUBMITTED
FOR THE DEGREE OF MASTER OF SCIENCE
DEPARTMENT OF BIOLOGICAL SCIENCES
NATIONAL UNIVERSITY OF SINGAPORE**

2009

Acknowledgements

I am deeply grateful for all the great scientific advices and endless support from my advisor, Prof. Wong Sek Man. I would not have come this far without his continuous encouragement. Especially, this dissertation would never have finished without his great contributions.

I would also like to thank Dr. Seow Teck Keong and Dr. Lin Qingsong for their invaluable help and professional support. Also, I would like to express my heartfelt gratitude to Cheryl Chan for her help on the 2-DE techniques. In addition, I would like to extend my gratefulness toward my fellow lab members: Dr. Niu Shengniao, Qiao Yan, Zhang Xin, Sunil Kumar Tewary and the lab officer Chong Ping Lee.

Further, I really appreciate my fellow classmates, and other members of the Department of Biological Sciences who always kindly give me a hand when I need one. All experiences I acquired from all the time I have been a part of Molecular Virology lab will always be the most valuable treasure of my life.

I would also acknowledge the financial support of National University of Singapore. Most importantly, no word can describe my eternal gratitude toward my Mom and Dad; their absolute belief in me is what keeps me motivated to complete the grandest task of my life. I would also like to thank all of my family and friends who always cherish my success and give me strength when I need it most.

Table of Contents

Acknowledgements	I
Table of Contents	II
Summary	VI
List of Tables	i
List of Figures.....	i
List of abbreviations	ii

Chapter 1. Introduction

1.1 Turnip crinkle virus (TCV).....	1
1.1.1 Viral genome.....	1
1.1.2 Structure and functions of coat protein.....	1
1.2 TCV infection mechanisms and host-virus interactions	2
1.3 Proteomics and advances in plant proteome	3
1.3.1 Proteomics and its various applications	3
1.3.2 Advances in plant proteome	4
1.4 Two-dimensional electrophoresis (2-DE) method and mass spectrometry (MS) analysis.....	4
1.4.1 2-DE method	5
1.4.2 MS analysis	5
1.5 Real-time PCR method	6

1.6	Objectives	7
-----	------------------	---

Chapter 2. General materials and methods

2.1	Plant materials.....	8
2.2	Preparation and inoculation of plants	8
2.3	Isolation of protoplasts.....	8
2.4	Isolation of chloroplasts.....	9
2.5	Western blot analysis	10
2.6	Protein extraction	11
2.6.1	Extraction of total proteins from protoplasts	11
2.6.2	Extraction of membrane proteins from chloroplasts.....	11
2.7	Protein assay	12
2.8	2-DE of proteins from protoplasts or chloroplasts	13
2.8.1	Rehydration of immobilized pH gradient (IPG) Strips.....	13
2.8.2	Isoelectric focusing (IEF).....	13
2.8.3	Sodium dodecyl sulfate polyacrylamide gel electrophoresis (SDS-PAGE)	14
2.8.4	Silver Staining.....	14
2.9	In-gel digestion and purification of digested peptide samples.....	15
2.9.1	In-gel digestion.....	15
2.9.2	Zip-tip® purification	16

2.10	MS analysis of 2-DE spots	17
2.11	Real-time PCR analysis	18
2.11.1	Plant RNA extraction	18
2.11.2	cDNA synthesis and amplification	18
2.11.3	Real-time PCR analysis of mRNA	19
2.12	DNA sequencing	19
Chapter 3.	Presence of TCV coat protein in protoplasts and chloroplasts from infected <i>Nicotiana benthamiana</i> leaves	
3.1	Introduction	20
3.2	Results	21
3.2.1	Inoculation of <i>N. benthamiana</i> and western blot analysis	21
3.2.2	Protoplasts isolation and western blot analysis	21
3.2.3	Chloroplast isolation and western blot analysis	22
3.3	Discussion	22
Chapter 4.	2-DE of proteins extracted from protoplasts of non-infected versus TCV-infected <i>Nicotiana benthamiana</i> leaves	
4.1	Introduction	27
4.2	Results	28
4.2.1	Extraction of total proteins from protoplasts	28
4.2.2	2-DE of protoplast proteins	28
4.2.3	Identification of differentially expressed proteins	33

4.3 Discussion	37
Chapter 5. 2-DE of proteins extracted from chloroplasts of non-infected versus TCV-infected <i>Nicotiana benthamiana</i> leaves	
5.1 Introduction	48
5.2 Results	49
5.2.1 Isolation of chloroplasts and western blot analysis	49
5.2.2 Extraction of total proteins from chloroplasts	49
5.2.3 2-DE of chloroplast proteins and protein expression profile	53
5.2.4 Identification of differentially expressed proteins in the chloroplast	53
5.3 Discussion	53
Chapter 6. Real time PCR of RuBisCO gene in non-infected versus TCV-infected <i>Nicotiana benthamiana</i> leaves	
6.1 Introduction	61
6.2 Results	62
6.2.1 Synthesis of Real-time PCR primers and cloning of the RuBisCO gene fragment	62
6.2.2 Real-time PCR of RuBisCO	62
6.3 Discussion	62
Literature cited	67

Summary

Turnip crinkle virus (TCV) and *Nicotiana benthamiana* are valuable models to investigate virus-host interaction. The detailed mechanisms of TCV replication and systematic movement in host plants are still not clear. To further understand the processes, two-dimensional electrophoresis (2-DE) coupled with mass spectrometry were used to reveal differentially expressed proteins from isolated protoplasts and chloroplasts of non-infected and TCV-infected *N. benthamiana* leaves.

Fifteen differentially expressed proteins were identified and 8 were up-regulated, while 7 were down-regulated. These proteins were mainly involved in photosynthesis (RuBisCO, RuBisCO activase, chlorophyll a/b binding protein and ferredoxin-NADP reductase), stress response and detoxification (zinc protease, ascorbate peroxidase and heat shock protein 70), energy metabolism (adenylate kinase and ATP synthase), maintenance of pH (chloroplast carbonic anhydrase) and TCV coat protein. Real-time PCR results showed a down-regulation by 62% in TCV-infected *N. benthamiana* leaves, which confirmed the 2-DE results.

In summary, TCV inhibits certain pathways and affects key functions of the plants such as photosynthesis and transcription. Plants resist by increasing protein degradation and detoxification. The 2-DE results of this study have provided us with a more comprehensive picture of plant virus-host interactions and have shed some light on the mechanism of virus infection. (195 words)

List of Tables

- Table 4.1 Differentially Expressed Proteins between TCV-infected and non-infected *N. benthamiana* protoplast protein.
- Table 4.2 Proteins identified with differential expression in *N. benthamiana* protoplasts with TCV infection.
- Table 5.1 Differentially Expressed Proteins between TCV-infected and non-infected *N. benthamiana* chloroplast proteins.
- Table 5.2 Proteins identified with differential expression in *N. benthamiana* with TCV infection.
- Table 6.1 Ct values of the Real-time PCR
- Table 6.2 Comparison of RuBisCO large subunit gene expression in TCV-infected *N. benthamiana* with non-infected *N. benthamiana*.

List of figures

- Figure 1.1 TCV genome structure.
- Figure 3.1 Western blot analyses of TCV-infected *N. benthamiana* leaves and protoplasts using anti-TCV CP antibodies.
- Figure 3.2 Western blot analyses of TCV-infected chloroplasts from *N. benthamiana* leaves using anti-TCV CP antibody.
- Figure 3.3 Western blot analyses of TCV-infected *N. benthamiana* leaves with different wpi using antibodies against TCV CP.
- Figure 4.1 Standard curve s of protein quantification assay.
- Figure 4.2 2-DE gels of non-infected *N. benthamiana* and TCV-infected *N. benthamiana* leaf protoplast protein.
- Figure 4.3 A representative 2-DE map of proteins extracted from protoplasts of non-infected *N. benthamiana* leaves and analysis of the proteome profile.
- Figure 4.4 A representative 2-DE map of proteins extracted from protoplasts of TCV-infected *N. benthamiana* leaves the analysis of the proteome profile.

- Figure 4.5 Protein spots with significant change.
- Figure 4.6 The pathways that virus affects in plant.
- Figure 5.1 Standard curve of the protein quantification assay.
- Figure 5.2 A representative 2-DE map of proteins from chloroplasts of non-infected *N. benthamiana* and the analysis of the proteome profile.
- Figure 5.3 A representative 2-DE map of proteins from chloroplasts of TCV-infected *N. benthamiana* and the analysis of the proteome profile.
- Figure 5.4 A representative 2-DE map of proteins from TCV-infected *N. benthamiana* chloroplasts and the analysis of the proteome profile.
- Figure 6.1 Comparison of RuBisCO large subunit gene expressions in non-infected versus TCV-infected *N. benthamiana*.

List of abbreviations

2-DE	two-dimensional electrophoresis
ACN	acetonitrile
APS	ammonium persulfate
BCIP	5-bromo-4-chloro-3-indolyl phosphate
BSA	bovine serum albumin
CHCA	α -cyano-4-hydroxycinamic acid
CHAPS	3-[(3-Cholamidopropyl) dimethylammonio]-1-propanesulfonate
CP	coat protein
Ct	cycle threshold
DTT	dithiothreitol
EDTA	ethylenediaminetetraacetic acid

HSP	heat shock proteins
IAA	iodacetate
IEF	isoelectric focusing electrophoresis
IPG	immobilized pH gradient
MALDI	matrix-assisted laser desorption/ionization
MS	mass spectrometry
MS/MS	tandem mass spectrometry
NBT	nitro blue tetrazolium
NCBI	national centre for biotechnology information
NCBI nr database	NCBI nonredundant database
PBS	phosphate buffered saline
PCD	programmed cell death
PCR	polymerase chain reaction
RCA	RuBisCO activase
ROS	reactive oxygen species
RuBisCO	ribulose-1, 5-bisphosphate carboxylase oxygenase
RuBP	ribulose-1, 5-bisphosphate
SDS	sodium dodecyl sulfate
TCV	turnip crinkle virus
TEMED	N, N, N', N'-tetramethylethylenediamine
TFA	trifluoroacetic acid

TIP	TCV interacting protein
TPI	triose phosphate isomerase
wpi	week postinoculation

CHAPTER 1. INTRODUCTION

1.1 Turnip crinkle virus (TCV)

Turnip crinkle virus (TCV) is a plant virus that belongs to the family of Tombusviridae and genus of Carmovirus. It has a wide host range which primarily consists of many members of the Brassicaceae family. Symptoms of TCV infection on plants are local chlorotic lesions, systemic leaf mottling and crinkling (<http://www.ictvdb.rothamsted.ac.uk/ICTVdB/>).

1.1.1 Viral genome

TCV genome consists of a single-stranded, positive sense RNA molecule of 4054 nucleotides. This single RNA molecule encodes five proteins (Carrington *et al.*, 1989) (Figure 1.1).

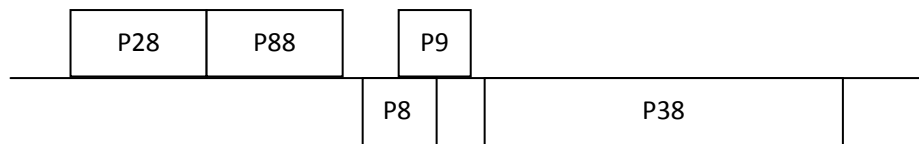


Figure 1.1: TCV genome structure. The five open reading frames of TCV are: p28 and its readthrough product p88, responsible for viral replication; p8 and p9, required for viral movement; and p38, the coat protein.

1.1.2 Structure and functions of coat protein

The P38 protein translated from subgenomic RNA of TCV genome is a viral coat protein. It consists of 180 capsid protein subunits which make up to a total molecular weight of 38 kDa (Carrington *et al.*, 1987). TCV coat protein can be divided into three main structural domains namely R (RNA-binding), S (shell), and P (protruding)

domain (Hogle *et al.*, 1986).

TCV coat protein is a multifunctional protein. Primarily, it acts as a structural protein in forming the virion. Besides, TCV coat protein also acts as a strong suppressor of RNA silencing. The 25-amino-acid fragment located at the N-terminus of its coat protein plays a vital role in suppressing RNA silencing (Thomas *et al.*, 2003). A study has suggested that the coat protein functions by suppressing a Dicer-like RNase found in plant cells (Qu *et al.*, 2003).

1.2 TCV infection mechanisms and host-virus interactions

The mechanism that TCV replicates and systematically moves in the host plant is still not clear. However, the coat protein plays an important role in the infection and systematic movement (Kong *et al.*, 1997). Point mutations in the coat protein can alter its secondary structure and affect the host-plant interaction (Lin & Heaton, 1999). Recent research also revealed that short internal sequences in a subviral RNA were involved in replication (Sun *et al.*, 2005). Besides, two nuclear localization signals on p8 proved its nuclear localization and p8 also facilitated cell-to-cell movement of the virus (Cohen *et al.*, 2000).

Moreover, TCV-interacting protein (TIP) was discovered in *Arabidopsis* and the nuclear localization of TIP was blocked by the coat protein (Ren *et al.*, 2005). Furthermore, *Arabidopsis* Di-17 is resistant to TCV infection as the N-terminus of the coat protein was an avirulent factor (Zhao *et al.*, 2000).

1.3 Proteomics and advances in plant proteome

1.3.1 Proteomics and its applications

Proteins are the major executors of biological functions. Proteomics has been brought forward since 1996 with the intention of bridging the knowledge gap between genomes and living cells (Marc Wilkins *et al.*, 1996). It is increasingly becoming more popular after the genomics wave. Similar to genomics, proteomics is also a form of systematic and large-scale analysis. However, instead of analyzing gene sequences, proteins are analyzed. Compared with the cellular genome, the proteome is dynamic and changes with time. Each cell or tissue type has its unique proteome even in the same organism. Moreover, the proteome changes in response to alteration of environmental conditions. The study of the dynamic proteomes has the potential to reveal new targets for intervention in disease processes (Persidis & Ze, 1998).

Although proteomics has only been developed for less than fifteen years, it has many applications. Firstly, it can be used to annotate genomes, resulting in a better understanding of gene function and regulation (Hollywood *et al.*, 2006). Secondly, it is useful in studying protein post-translational modifications (Kwon *et al.*, 2006). Thirdly, it was widely applied to further understand protein localization and compartmentalization. Besides, proteomics is used to screen for protein-protein interactions (Berggard *et al.*, 2007). It also has the advantage in providing data in protein expression for example, perturbation of biological systems and disease progression.

Proteome analysis consists of three main steps: separation, identification, and quantification of proteins from biological samples. It includes both experimental techniques and application of bioinformatics.

1.3.2 Advances in plant proteomic analyses

With the accumulation of genomic data, proteomics is increasingly important for the study of plant functions. Proteome analysis sheds new light on the complex mechanisms of plant growth, development and interactions with the environment.

The dominant analytical platform of proteomics has been the two-dimensional gel electrophoresis (2-DE) coupled to MS (Rossignol *et al.*, 2006). As a powerful tool, 2-DE offers high resolution and rapid development in data analysis software and MS hardware has made MS the preferred method for protein identification (Saravanan & Rose, 2004). Besides, techniques such as difference gel electrophoresis, isotope-coded affinity tags and stable isotope labeling of peptides and proteins are also used as alternatives (Julka & Regnier, 2004).

However, there are still several challenges because plant cells are usually rich in proteases and they contain rigid cell walls, polysaccharides and various secondary compounds (Canovas *et al.*, 2004). In addition, certain tissues contain some abundant proteins that are so dominant in protein samples that the detection of other low abundant proteins are quenched (Chen & Harmon, 2006).

1.4 2-D electrophoresis method and mass spectrometry analysis

2-DE coupled to MS constitutes an important platform utilized in plant proteome

analysis. They are widely used to analyze proteins and screen the proteome.

1.4.1 2-D electrophoresis method

The 2-DE is a form of gel electrophoresis that was first developed by O'Farrell (O'Farrell, 1975) and Klose (Klose, 1975a) in 1975. It is one of the leading techniques to separate individual proteins and document the patterns of gene expression in biological samples.

2-DE separates the proteins by two properties in two dimensions. In the first dimension, proteins are separated according to different isoelectric points by isoelectric focusing electrophoresis (IEF). The introduction of immobilized pH gradient (IPG) greatly increased the sensitivity and lowered the discrepancies between calculated and experimental *pI* values to 0.001 pH units (Bjellqvist *et al.*, 1994). In the second dimension, protein molecules are separated on the basis of their molecular mass. The theoretical resolution has reached 10,000 spots per 2-D gel.

2-DE can investigate thousands of proteins simultaneously from very small amount of material. Unlike liquid chromatography in proteomics which mainly performs analysis on peptides, 2-DE reveals a whole map of intact proteins, thus providing the information of the changes in protein expression levels, isoforms and post-translational modifications (Görg *et al.*, 2004). The 2-DE spot patterns also enable the creation of a 2-D image databases.

1.4.2 Mass spectrometry analysis

The MS first generates charged molecules and then measures their

mass-to-charge ratios. With the introduction of two ionization methods: electrospray ionization (Fenn *et al.*, 1989) and matrix-assisted laser desorption/ionization (MALDI), MS is a fast and effective method for the characterization of proteins. MS data can be matched with protein sequences in the databases and protein structures and functions can be predicted (Henzel *et al.*, 1993).

With the development of the detector and the ionization techniques, MS is much more sensitive and is able to deal with more complex samples. Furthermore, the precursor-ion selection module of tandem mass spectrometry (MS/MS) (Biemann, 1988) can effectively isolate a single peptide (or a few peptides with the same m/z) from a complex mixture and remove the contribution of most other peptides to the sequence-analysis step. Moreover, with peptide mass fingerprint, proteins can be identified and recognized very quickly by comparing the fingerprinting patterns with the databases (Breitling *et al.*, 2006).

1.5 Real-time polymerase chain reaction (PCR) method

Real-time PCR (or quantitative real time PCR) is based on the method of PCR but the amount of DNA is monitored during the process of PCR. It was first developed by Higuchi and associates (Higuchi *et al.*, 1993) and is now widely used.

Real-time PCR measures the time the fluorescent signal takes to reach the threshold and the fluorescent intensity is correlated with the amount of DNA. Therefore, the amount of starting DNA can be calculated even if it is very small. Furthermore, reverse transcription can be used with real-time PCR so that the RNA levels in the

cells can be measured (Bustin, 2000).

Real-time PCR has several advantages. Firstly, it is very sensitive in the detection of DNA at extraordinarily low levels of expression. Secondly, it is precise enough to detect subtle gene expression changes (Luu-The *et al.*, 2005). Moreover, compared with the time consuming northern blot, real-time PCR is relatively quick.

1.6 Objectives

1. To identify differentially expressed proteins between TCV-infected and non-infected *N. benthamiana* leaves using 2-DE and MS.

2. To analyze gene expression in TCV-infected and non-infected *N. benthamiana* using real-time PCR in order to understand the effects of TCV infection on plant host at transcriptional level.

3. To investigate the host response to TCV infection and to understand the mechanism(s) of virus-host interaction.

CHAPTER 2. GENERAL MATERIALS AND METHODS

2.1 Plant materials

Nicotiana benthamiana was used as the host plant for systemic infection and as the starting material for protoplast production. All *N. benthamiana* plants were grown in the greenhouse under 16 h light/8 h dark at 25°C.

2.2 Preparation and inoculation of plants

About 0.5 g TCV-infected leaves were ground using inoculation buffer (0.05 M sodium phosphate, pH 5.8) and mixed with a small amount of carborundum. *N. benthamiana* with 6-8 leaves were mechanically inoculated with the inoculum as described above. The inoculated plants were kept in the dark for 16 h.

2.3 Isolation of protoplasts

Fully expanded leaves were harvested from 3 weeks old *N. benthamiana* plants. The leaves were surface sterilized in 0.8% Clorox[®] (5.25% sodium hypochlorite) for 10 min with constant agitation and washed with RO water for 3 times, 5 min each. The leaves were sliced into 1 mm strips and immediately put into an enzyme mixture [0.5 M mannitol, 22 mM KNO₃, 0.5 mM MES, 1 μM KI, 10 mM CaCl₂, 0.1 μM CuSO₄, 0.75 mM KH₂PO₄, 0.5% cellulase R10 and 1% macerozyme R10 (Yakult Honsha, Japan), pH 5.7]. The mixture was then incubated for 8-10 h at 25°C in the dark.

The protoplast mixture was gently siphoned up and down using a sterile pipette

until most protoplasts were released into the enzyme solution. The suspension was then filtered through 70 μm nylon screen to remove the debris. The filtrate was centrifuged at 100 g for 3 min, and the supernatant was removed carefully. The protoplasts were gently resuspended in washing solution (10 mM HEPES, 150 mM NaCl, 0.5 M Mannitol, 10 mM CaCl_2 , pH 5.7) and centrifuged at 100 g for 3 min. The protoplasts were washed and collected as described above until the supernatant became clear and were suspended in 4 ml washing solution.

First 10 μl of the final suspension was taken out and diluted to 1 ml. The protoplasts were counted using the light microscope. Then the concentration and amount of the protoplasts were calculated.

2.4 Isolation of chloroplasts

Plants were placed in the dark for 24-36 h before the leaves were collected. Five grams of young green leaves were rinsed in cold 5% Clorox® for 4 min and washed with cold water for 3 times. The veins were cut off and the leaves were sliced into strips. Then they were blended in 30 ml isolation buffer [350 mM sorbitol, 50 mM Tris-HCl (pH 8.0), 5 mM EDTA, 0.1% BSA (w/v), 0.1% β -mercaptoethanol (v/v), 0.1% sodium ascorbate (w/v)]. The homogenate was filtered through the sieve and 70 μm nylon screens. Then the mixture was centrifuged with 3,000 g for 15 min at 4°C. The green pellet was resuspended in 5 ml washing buffer (350 mM sorbitol, 50 mM Tris-HCl (pH 8.0), 20 mM EDTA) and applied to a sucrose gradient (30%/45%/60%) with the top covered by 1 ml washing buffer. The sucrose gradient with sample was

centrifuged with 25,000 rpm for 1 h at 4°C. The dark green chloroplast band was aspirated and washed by 30 ml washing buffer. The resuspension was centrifuged with 6,000 g for 10 min at 4°C. Then the pellet was resuspended in 5 ml washing buffer.

2.5 Western blot analysis

The protein samples were mixed with 6×loading buffer [0.1 M Tris-HCl (pH 6.8), 20% glycerol (v/v), 4% sodium dodecyl sulfate (SDS) (w/v), 5% β-mercaptoethanol (v/v), 0.2% bromophenol blue (w/v)] and heated for 5 min in boiling water bath. Then they were loaded on SDS-polyacrylamide gel (12% separating gel: 1.6 ml water, 2.0 ml 30% acrylamide, 1.3 ml 1.5 M Tris-HCl (pH 8.8), 50 μl 10% SDS, 50 μl 10% ammonium persulfate (APS), 2 μl N, N, N', N'-tetramethylethylenediamine (TEMED)); 5% stacking gel: 1.36 ml water, 330 μl 30% acrylamide, 250 μl 1 M Tris-HCl (pH 6.8), 20 μl 10%SDS, 20 μl 10% APS, 2 μl TEMED). The electrophoresis was conducted with running buffer (25 mM Tris base, 192 mM glycine, 0.1% SDS) at 100 V for 2 h.

A suitable size of nitrocellulose membrane (GE Healthcare) was cut and wet in the transfer buffer (10% methanol, 0.01 M Tris base, 0.096 M glycine). Pre-wet sponges and filter papers were assembled with the gel and the membrane. The transferring was conducted in the mini-transblot (Bio-rad) at 100 V for at least 1 h with the cold pack.

The membrane with proteins was immediately immersed in blocking buffer (5%

non-fat milk powder in phosphate buffered saline (PBS) buffer (10 mM sodium phosphate, pH7.2, 0.9% (w/v) NaCl). After incubation for 1 h at room temperature or overnight at 4 °C, the membrane was transferred into 10 ml PBS buffer with primary antibody and incubated for 1 h at 25°C with constant shaking. The membrane was washed by PBS buffer for 10 min, 3 times before transferred into 10 ml PBS buffer with secondary antibody. After incubation for 1 h, the membrane was washed by PBS buffer for 10 min, 3 times.

The membrane was developed in the freshly-made substrate [100 mM Tris-HCl, 100 mM NaCl, 5 mM MgCl₂ pH 9.5, 0.375 mg/ml nitro blue tetrazolium (NBT) (Sigma), 0.25 mg/ml 5-bromo-4-chloro-3-indolyl phosphate (BCIP) (Sigma)].

2.6 Protein extraction

2.6.1 Extraction of total proteins from protoplasts

Protoplasts were centrifuged at 100 g for 3 min. The supernatant was carefully removed and the pellet was transferred to a pre-chilled mortar. The pellet was homogenized in liquid nitrogen before the protein extraction buffer was added. The mixture was further ground to fine powder and was transferred to a new tube before being centrifuged at 200,000 g for 30 min at 10°C. The supernatant was transferred to a new tube and kept at -20°C.

2.6.2 Extraction of total proteins from chloroplasts

For 1 ml chloroplast suspension, 4 ml methanol was added. The mixture was vortexed and centrifuged for 10 s at 9000 g. Then the supernatant was transferred into

a new tube. After adding 1 ml water saturated chloroform, the sample was vortexed and centrifuged for 10 s at 9000 g. To separate the phase, 2 ml deionized water was added, and the sample was vortexed and centrifuged for 1 min at 9000 g. The upper phase (aqueous phase) was carefully removed and discarded, and then 3 ml methanol was added to precipitate the protein. After vortex, the mixture was centrifuged at 9000 g for 2 min. The supernatant was removed and the pellet washed with 1 ml 95% (v/v) methanol twice, then the pellet was lyophilized and stored at -80°C.

2.7 Protein assay

Protein samples were quantified using the 2-D Quant Kit (GE Healthcare). Different amounts of bovine serum albumin (BSA) standard solution (0-60 µg) were prepared according to manufacturer's instructions. Tubes containing 10 µl of the samples were prepared to be assayed.

First, 500 µl of precipitant reagent were added to each tube and incubated for 2 min with vortex mixing. Then 500 µl of co-precipitant reagent were added to each tube, mixed briefly, centrifuged at 12,000 g for 10 min and the supernatant was discarded. Copper solution (100 µl) and 400 µl distilled water were mixed into each tube. After the precipitated proteins were dissolved, 1 ml freshly-made working color reagent (color reagent A: color reagent B=100:1) was added into each tube and incubated at room temperature for 15 min.

The absorbance at 480 nm for each sample or standard solution was read. The standard curve was plotted according to the absorbance of BSA standard solutions

and protein concentration was estimated.

2.8 2-D electrophoresis of proteins from plant leaves and protoplasts

2.8.1 Rehydration of IPG Strips

First, 340 μ l IPG rehydration buffer solution (7 M urea, 2 M thiourea, 2% 3-[(3-Cholamidopropyl)dimethylammonio]-1-propanesulfonate (CHAPS), 20 mM dithiothreitol (DTT), 0.5% IPG buffer, 0.002% bromophenol blue) was loaded to each well of the Dry Strip Tray (Amersham Bioscience). The 18 cm pH 3-10 IPG strip was placed into the Dry Strip Tray with gel-surface facing downward. The strip was covered with 1 ml cover oil (Amersham Bioscience) and incubated for at least 10 h.

2.8.2 Isoelectric focusing

The rehydrated strip was taken out of the Dry Strip Tray and put into the ceramic tray with gel-surface facing up. Two Milli-Q water dampened paper bridges were applied at both ends of the strip. The electrodes were placed onto the paper bridges to enable electrical connection. The loading cup was applied onto the gel near the positive electrode. After the tray was placed on the Ettan IPGphor 3 (GE Healthcare), 60 μ l sample solution (7 M urea, 2 M thiourea, 2% CHAPS, 20 mM DTT, 0.5% IPG buffer, 0.002% bromophenol blue) with 100 μ g protein was loaded to the loading cup. Then 3 ml cover oil was applied on the gel and the lid of the Ettan IPGphor 3 was closed before starting the IEF. The program for IEF was set as follows: 200 V for 30 min, 500 V for 30 min, 1000 V for 30 min, 1000-8000 V (gradient) for 30 min and 8000 V for 3.5 h. After that the IPG strip was harvested and kept at -80 °C.

2.8.3 Sodium dodecyl sulfate polyacrylamide gel electrophoresis (SDS-PAGE)

The IPG strip was soaked in 10 ml DTT equilibration buffer (6 M urea, 75 mM Tris-HCl (pH 8.8), 29.3% glycerol, 2% SDS, 0.002% bromophenol blue, 1% DTT) for 15 min. Then the strip was transferred to 10 ml iodoacetate (IAA) equilibration buffer (6 M urea, 75 mM Tris-HCl (pH8.8), 29.3% glycerol, 2% SDS, 0.002% bromophenol blue, 2.5% IAA) for 15 min with constant shaking.

After equilibration the strip was loaded onto a SDS-PAGE gel (22cm×20cm, 12.5%: 14.52 ml double-distilled water, 14.68 ml 30% acrylamide, 10 ml 1.5 M Tris-HCl (pH8.8), 400 µl 10% SDS, 20 µl TEMED, 400 µl 10% APS) and sealed with sealing solution (25 mM Tris base, 192 mM glycine, 0.1% SDS, 0.5% agarose, 0.002% bromophenol blue). Protein marker was loaded at the end of the strip.

The gel set was put into the vertical SDS-PAGE tank filled with SDS running buffer (25 mM Tris base, 192 mM glycine, 0.1% SDS). The program was set and the electrophoresis was conducted at 10 °C for 40 min at 15 mA/strip and 4 h at 30 mA/strip. Then the polyacrylamide gel was harvested and put into the staining basin.

2.8.4 Silver Staining of 2D Gels

The gel was immersed in fix solution (50% methanol, 12% Acetic acid, 0.05% formalin) for at least 12 h. Then it was washed with washing solution (35% ethanol) for 20 min, 3 times. After washing, the gel was transferred to sensitizing solution (0.02% Sodium thiosulphate) for 2 min and washed with Milli-Q water for 3 times,

each time 1 min. The gel was incubated in staining solution (0.2% silver nitrate, 0.076% formalin) for 20 min with constant shaking. Followed by washing with Milli-Q water for 2 times, each time 1 min, the gel was developed in developing solution (6% sodium carbonate, 0.05% formalin, 0.0004% sodium thiosulphate). After the spots appeared on the gel, stop solution (1.46% ethylenediaminetetraacetic acid (EDTA)) was added to stop the developing reaction.

2.9 In-gel digestion and Zip-tip[®] purification

2.9.1 In-gel digestion

Each spot was cut from the gel and put into individual microfuge tubes. Washing buffer (150 μ l) consisting 2.5 mM NH_4HCO_3 , 50% acetonitrile (ACN) was added and the tubes were sealed with parafilm and kept overnight at 4°C. After incubation, the washing buffer was removed and 150 μ l freshly made washing buffer was added. The mixture was vortexed and kept at 37°C for 10 min with constant shaking. The washing buffer was removed and the gel pieces were dried under vacuum in a Savant Speed Vac.

First, 20 μ l freshly made DTT solution (10 mM DTT, 100 mM NH_4HCO_3) was added to the dried gel pieces and the mixture was incubated for 1 h at 56°C with constant shaking. Then the gel pieces were treated with 20 μ l freshly-made IAA solution (55 mM IAA, 100 mM NH_4HCO_3) for 45 min at room temperature. The tubes were kept in the dark with constant shaking.

The gel pieces were treated with 100 μ l of 100 mM NH_4HCO_3 at 37 °C for 10

min, followed by incubation with 100 μl ACN at room temperature for 10 min. This step was repeated for 3 times and the gel pieces were vacuum dried. An aliquot of 10 μl trypsin solution (0.01 $\mu\text{g}/\mu\text{l}$ trypsin, 50 mM NH_4HCO_3) was added to each tube and incubated at 4°C for 30 min. The trypsin solution was removed and 10 μl 25 mM NH_4HCO_3 was added. The tubes were sealed with parafilm and incubated at 37°C for 16 h.

The mixture was centrifuged at 6,000 g for 10 min and the supernatant was transferred into new tubes. Then 10 μl freshly-prepared 0.1% trifluoroacetic acid (TFA) in 50% ACN was added into each tube before the tubes were sealed with parafilm. The mixture was sonicated in a water-bath sonicator for 15 min. Then it was centrifuged at 6,000 g for 10 min and the supernatants were collected and combined. The peptide solution was dried under vacuum and the pellet was washed with 50% ACN twice. The samples were stored at -20°C.

2.9.2 Zip-tip® purification

The samples were dissolved in 0.1% TFA. Firstly, 10 μl wetting solution (50% ACN) was aspirated and dispensed for 5 cycles to wet the column. Secondly, 10 μl double distilled water was aspirated and dispensed for 5 cycles to equilibrate the column. After that 10 μl sample solution was aspirated and dispensed for 10 cycles to bind the peptides with the column. Then 10 μl double distilled water was aspirated and dispensed for 5 cycles to wash the column. Thirdly, 5 μl elution buffer (0.1% TFA, 50% ACN) was aspirated and dispensed for 5 cycles to elute the samples.

Finally, the samples were dried under vacuum.

2.10 Mass spectrometry analysis

Firstly, 0.5 μ l sample solution was mixed with 0.5 μ l matrix solution (10 mg/ml α -cyano-4-hydroxycinnamic acid (CHCA), 0.1% TFA, 50% ACN) and spotted onto a MALDI target plate (Applied Biosystems). After the plate was loaded into the ABI 4700 Proteomics Analyzer MALDI-TOF/TOF mass spectrometer (Applied Biosystems), MS spectra were obtained with 1,000 laser shots per spectrum. Six external standards (mass standard kit for the 4700 Proteomics Analyzer calibration mixture, Applied Biosystems) spotted at the corners/edges of the MALDI target plate were used for plate calibration to ensure a mass accuracy within 50 ppm.

After that, up to ten most intense ions from each MS spectrum were selected for MS/MS. The MS/MS analyses were performed using air, at collision energy of 1 kV and a collision gas pressure of 1×10^{-6} Torr. The MS/MS data were acquired with stop conditions so that 3,000-6,000 laser shots were combined for each spectrum. For MS/MS spectra that matched to certain peptide sequences but the MASCOT search (see below) results were not significant enough, more laser shots were manually acquired to improve the quality of the spectra.

All of the MS and MS/MS spectra were combined to search against the National Centre for Biotechnology Information (NCBI) nonredundant database (NCBI nr database, 7614964 sequences) using the software GPS ExplorerTM Version 3.6 and MASCOT 2.1 (Matrix Science). One missing cleavage was allowed and cysteine

carbamidomethylation, N-terminal acetylation and methionine oxidation were selected as variable modifications. Peptide mass tolerance was set to 150 ppm and fragment error tolerance was set to ± 0.4 Da. Maximum peptide rank and minimum ion score C.I% (peptide) were set to 2 and 50 respectively.

2.11 Real-time PCR analysis

2.11.1 Plant RNA extraction

Plant tissue sample (100 mg) was homogenized with liquid nitrogen and added to 1 ml TRIzol[®] reagent (Invitrogen). The suspension was incubated for 5 min at room temperature before 200 μ l chloroform was added. The sample was then mixed vigorously by shaking for 15 s and then incubated at room temperature for 3 min. The aqueous phase was transferred to a new tube followed by centrifugation with 12,000 *g* for 10 min at 4 °C. RNA was precipitated by mixing 0.5 ml isopropanol with the aqueous phase. The sample was centrifuged with 12,000 *g* for 10 min at 4 °C followed by incubation at room temperature for 10 min. The pellet was washed with 1 ml 75% ethanol and centrifuged at 12,000 *g* for 1 min at 4 °C before it was dried and dissolved in RNase-free water.

2.11.2 cDNA synthesis and amplification

For each reverse transcription reaction, 1 μ g RNA, 2 μ l 5 \times RT buffer (Invitrogen), 0.8 μ l 10 mM dNTP, 0.2 μ l 50 units/ μ l Murine Leukemia Virus Reverse Transcriptase, 0.2 μ l 100 μ mol reverse primer of both of the actin gene and the ribulose-1,5-bisphosphate carboxylase oxygenase (RuBisCO) gene and 5.6 μ l H₂O

were added and mixed. The cDNA synthesis was then performed for 1 h at 42°C. The reaction was stopped by incubation at 80°C for 10 min.

2.11.3 Real-time PCR analysis of cDNA

Real-time PCR was carried out using the ABI 7700 (Applied Biosystems), according to the manufacturer's instructions. The mixture was denatured at 95°C for 10 min and 40 cycles of reactions were carried out. For each cycle of real-time PCR, the conditions were as follows: 95°C for 15 sec, and 60°C for 1 min. The cycle threshold (Ct) was recorded and the relative fold change was calculated based on the Ct value.

2.12 DNA sequencing

For one sequencing reaction, 10 µl mixture containing 0.25 µg of DNA template, 1.6 pmol of primer, and 4 µl of BigDye terminator reaction mixture (ABI PRISM™ Dye terminator Cycle Sequencing Ready Reaction Kit) was made and vortexed fully. The sequencing reaction was performed on the GeneAmp PCR machine for 25 cycles and each cycle was as follows: 96 °C for 10 sec, 50 °C for 5 sec, 60 °C for 4 min; rapid thermal ramp to 4 °C and hold. The mixture after the reaction was precipitated by ethanol and was dried under vacuum in a Savant Speed Vac. The sample was then run on the ABI PRISM 3100 automated sequencer.

CHAPTER 3. PRESENCE OF TCV COAT PROTEIN IN PROTOPLASTS AND CHLOROPLASTS FROM INFECTED *NICOTIANA BENTHAMIANA* LEAVES

3.1 Introduction

In order to search for the differentially expressed proteins involved in TCV infection, and to find out the general mechanism of the host-virus interaction, comparing proteins expressed in TCV-infected and non-infected *N. benthamiana* can be achieved by 2-DE analysis.

Protoplasts are cells with their cell walls removed. Protoplast isolation was first developed in 1960s (Cocking, 1960). It has wide-ranging applications including RNA transformation (Rathus & Birch, 1992), transient expression (Cormeau *et al.*, 2002; Teulieres *et al.*, 1991) and protoplast fusion (Ohgawara & Kobayashi, 1991). By expressing foreign genes, protoplast system is used to investigate the protein-protein interaction (Subramaniam *et al.*, 2001) and virus-host interaction (McLean *et al.*, 1995). Moreover, it is more convenient to extract the proteins from the protoplasts. Therefore, protoplast system is widely used in the plant proteomic study (Davey *et al.*, 2005).

Chloroplasts are bilayer membrane organelles and powerhouses in plants. They conduct photosynthesis by converting solar energy and carbon dioxide to oxygen and sugar. Photosynthesis is divided into two parts: light reactions and light-independent reactions (Calvin cycle). Without photosynthesis, there would be no life on earth.

Therefore, chloroplasts are very important as energy transformers.

In this Chapter, 3-week-old *N. benthamiana* was inoculated with TCV and the leaves were harvested after the virus made the systematic movement. The protoplasts and chloroplasts were isolated from *N. benthamiana* leaves using the method mentioned before. Presence of TCV CP in protoplasts and chloroplasts isolated from infected *N. benthamiana* leaves is confirmed by western blot analysis.

3.2 Results

3.2.1 Inoculation of *N. benthamiana* and western blot analysis

Chlorotic spots were observed on the inoculated leaves after 1 week post inoculation (wpi). With the virus movement, symptoms such as vein clearing and stunting appeared at 3 wpi. In addition, local lesions and leaf crinkling were also observed. The expression of TCV CP in *N. benthamiana* was confirmed by western blot (Figure 3.1 Lane 2).

3.2.2 Protoplasts isolation and western blot analysis

Protoplasts were isolated as mentioned in Chapter 2 and the concentration was calculated. A drop of protoplast suspension (10 µl) was loaded onto a haemocytometer and the number of cells was counted under the light microscope. The amount of protoplasts was calculated according to the concentration and the volume. For 2 g of *N. benthamiana* leaves, around 10^7 protoplasts could be harvested.

The existence of TCV CP is confirmed in *N. benthamiana* leaves and protoplasts; moreover, the amount of CP in protoplasts is even higher than that in leave tissue

(Figure 3.1 Lanes 2 & 4).

3.2.3 Chloroplast isolation and western blot analysis

Chloroplasts were isolated from *N. benthamiana* leaves using the method mentioned in Chapter 2. According to the western blot result (Figure 3.2), the existence of TCV CP is confirmed in the TCV-infected *N. benthamiana* chloroplasts.

3.3 Discussion

After inoculation, TCV CP gradually accumulated in the *N. benthamiana* as reflected by the western blot and the local lesion on the leaves. The amount of CP increased rapidly during the first 2 wpi and the increase was gradual after 2 wpi (Figure 3.3). After 4 wpi, the plant showed retarded growth and flowering. The leaves were not suitable for the 2-DE because of the presence of large amount of secondary metabolites.

Interestingly, the TCV CP transgenic *N. benthamiana* stopped showing visible symptoms after 4 wpi, suggesting that the CP-mediated resistance suppressed the virus replication. Moreover, because of the homologous expression of TCV-CP, the suppressor activity of TCV CP was silenced in the transgenic plants (Vasudevan *et al.*, 2008).

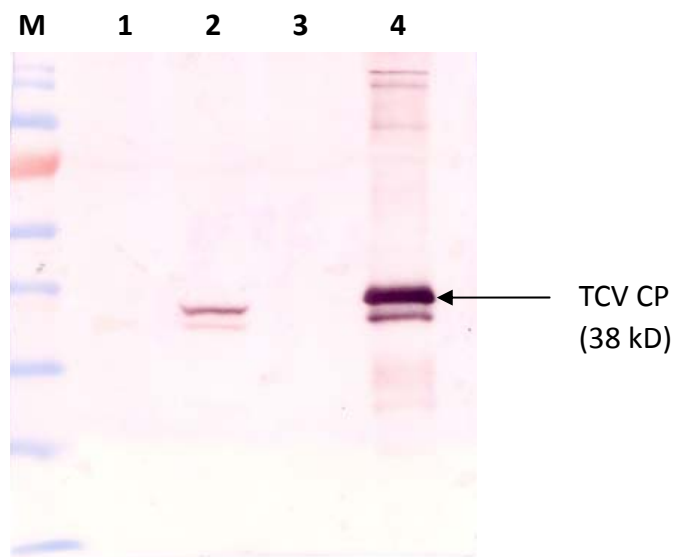


Figure 3.1 Western blot analyses of TCV-infected *N. benthamiana* leaves and protoplasts using anti-TCV CP antibody. M: Fermentas Page Ruler prestained protein ladder; lane 1: total protein from non-infected *N. benthamiana* leaves; lane 2: total protein from TCV-infected *N. benthamiana* leaves; lane 3: total protein from protoplasts of non-infected *N. benthamiana* leaves; lane 4: total protein from protoplasts of TCV-infected *N. benthamiana* leaves.

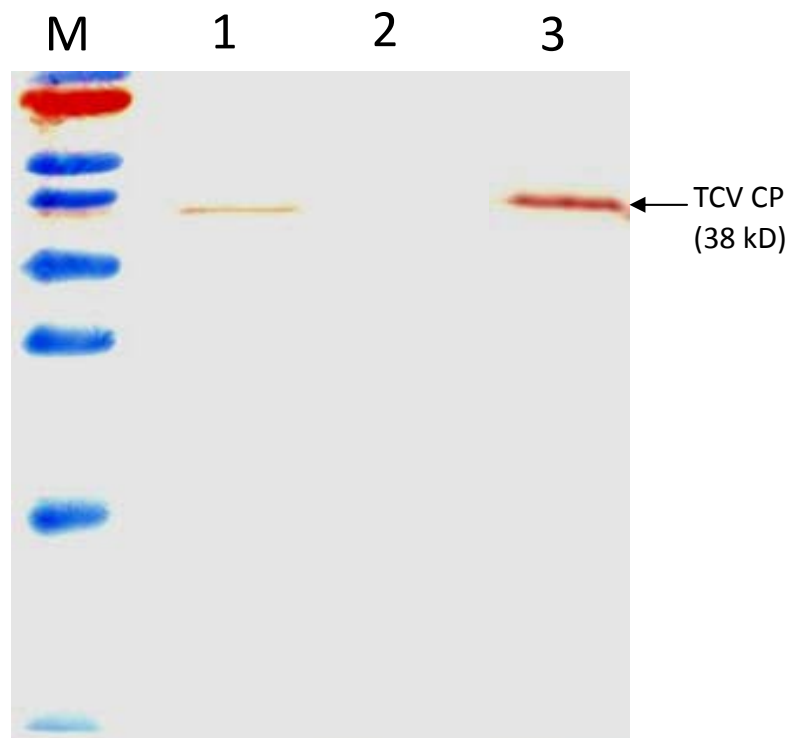


Figure 3.2 Western blot analyses of TCV-infected chloroplasts from *N. benthamiana* leaves using anti-TCV CP antibody. M: Fermentas Page Ruler prestained protein ladder; lane 1: protein from TCV-infected *N. benthamiana* leaves; lane 2: protein from non-infected *N. benthamiana* chloroplasts; lane 3: protein from TCV-infected *N. benthamiana* chloroplasts.

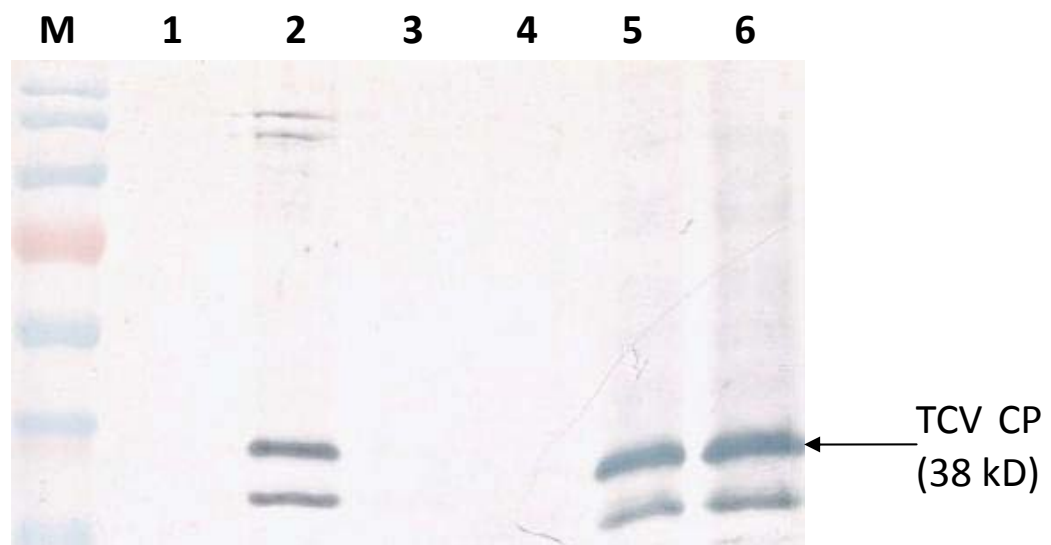


Figure 3.3 Western blot analyses of TCV-infected *N. benthamiana* leaves with different wpi using antibody against TCV CP. M: Fermentas Page Ruler Prestained Protein Ladder; lane 1: negative control (total protein from healthy *N. benthamiana* leaves); lane 2: Positive control (total protein from TCV-infected *N. benthamiana* leaves); lane 3: total protein from *N. benthamiana* leaves before TCV inoculation; lane 4: total protein from *N. benthamiana* leaves at 3dpi; lane 5: total protein from *N. benthamiana* leaves at 2wpi; lane 6: total protein from *N. benthamiana* leaves at 4wpi.

There was larger amount of CP present in the isolated protoplasts than TCV-infected *N. benthamiana* leaves (Figure 3.1 Lanes 2 & 4). It is probably due to less debris in the protoplasts because the cell wall was removed earlier. Furthermore, the protoplasts were easier to homogenize, thus alleviating protein degradation. Therefore, protoplast was a good experimental material for the 2-DE, as compared to the use of leaf tissues.

TCV coat protein is the structural and functional virus protein, and it also acts as a strong suppressor of RNA silencing. Therefore, western blot of TCV CP can reveal the virus amount in the host plants. Protein was extracted when the virus reached the largest amount in *N. benthamiana* leaves. The host-virus interaction would be most apparent in that stage.

The western blot showed two apparent bands and it is probably due to the degradation during the protein extraction. Thus during the sample preparation of the 2-DE, protease inhibitor mixture was used to minimize the degradation.

CHAPTER 4. 2-DE OF PROTEINS EXTRACTED FROM PROTOPLASTS OF NON-INFECTED VERSUS TCV-INFECTED *NICOTIANA BENTHAMIANA* LEAVES

4.1 Introduction

To find differentially expressed proteins between non-infected *N. benthamiana* and TCV-infected *N. benthamiana*, proteins extracted from the protoplasts need to be separated and compared. Since first developed in 1975 (Klose, 1975b; O'Farrell, 1975), 2-DE has become one of the standard procedures in proteomic research. It can provide the full network of a complete set of proteins in a given sample at a specified time (Issaq & Veenstra, 2008). With IPG of the IEF strips (Gorg *et al.*, 1988), separation of proteins were greatly improved. After several modifications (Gorg *et al.*, 2000; Klose & Kobalz, 1995) and combination with various staining methods (Patton, 2002), 2-DE has become a widely used method.

Furthermore, 2-DE combined with MS allows for the identification of the proteins in the cellular responses. With the development of the MS technique (Bjellqvist *et al.*, 1994) and more protein data entered into the databases, proteins can be identified more easily even without the whole genome information.

Firstly, total cellular proteins were extracted from the TCV-infected and non-infected *N. benthamiana* protoplasts. Then the expression patterns of the cellular proteins were obtained by 2-DE and silver staining. After that, comprehensive analyses of proteins associated with TCV infection were focused on the differentially expressed proteins. Finally,

protein spots with different intensities were processed for MS/MS analysis and the data were searched against NCBI database.

4.2 Results

4.2.1 Extraction of total proteins from protoplasts

Total cellular proteins were extracted using the method mentioned in Chapter 2 from TCV-infected and non-infected *N. benthamiana* protoplasts. A linear standard curve was obtained by plotting absorbance at 480 nm versus amount of BSA (Figure 4.1).

4.2.2 2-DE of protoplast protein

For TCV-infected and non-infected *N. benthamiana* protoplast protein, three biological replicates from both TCV-infected and non-infected *N. benthamiana* protoplasts were used and the 2-DE method was optimized to better separate the proteins. Proteins (100 µg) were first loaded onto a pH 3–10NL IPG strip for the first dimensional separation and then by 12.5% SDS-PAGE for the second dimensional separation. After that the resulting gels were stained with silver nitrate to reveal the protein spots. Each biological replicate was used twice to run the 2-DE. The developing time was 90s. The stained gels were scanned and compared (Figures 4.2, 4.3 and 4.4).

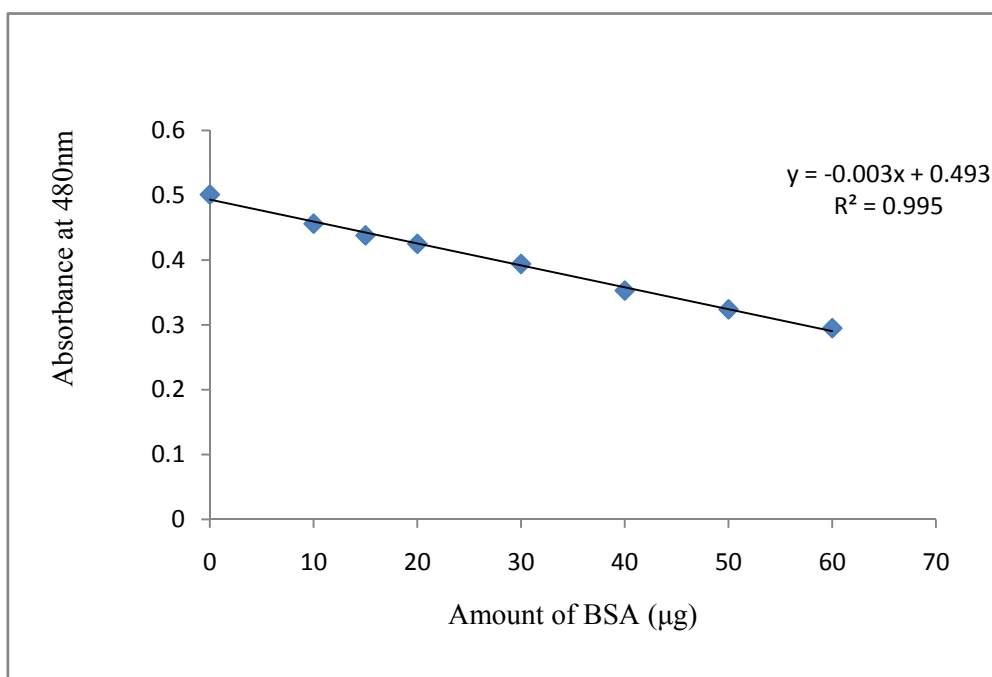


Figure 4.1 Standard curve s of protein quantification assay.

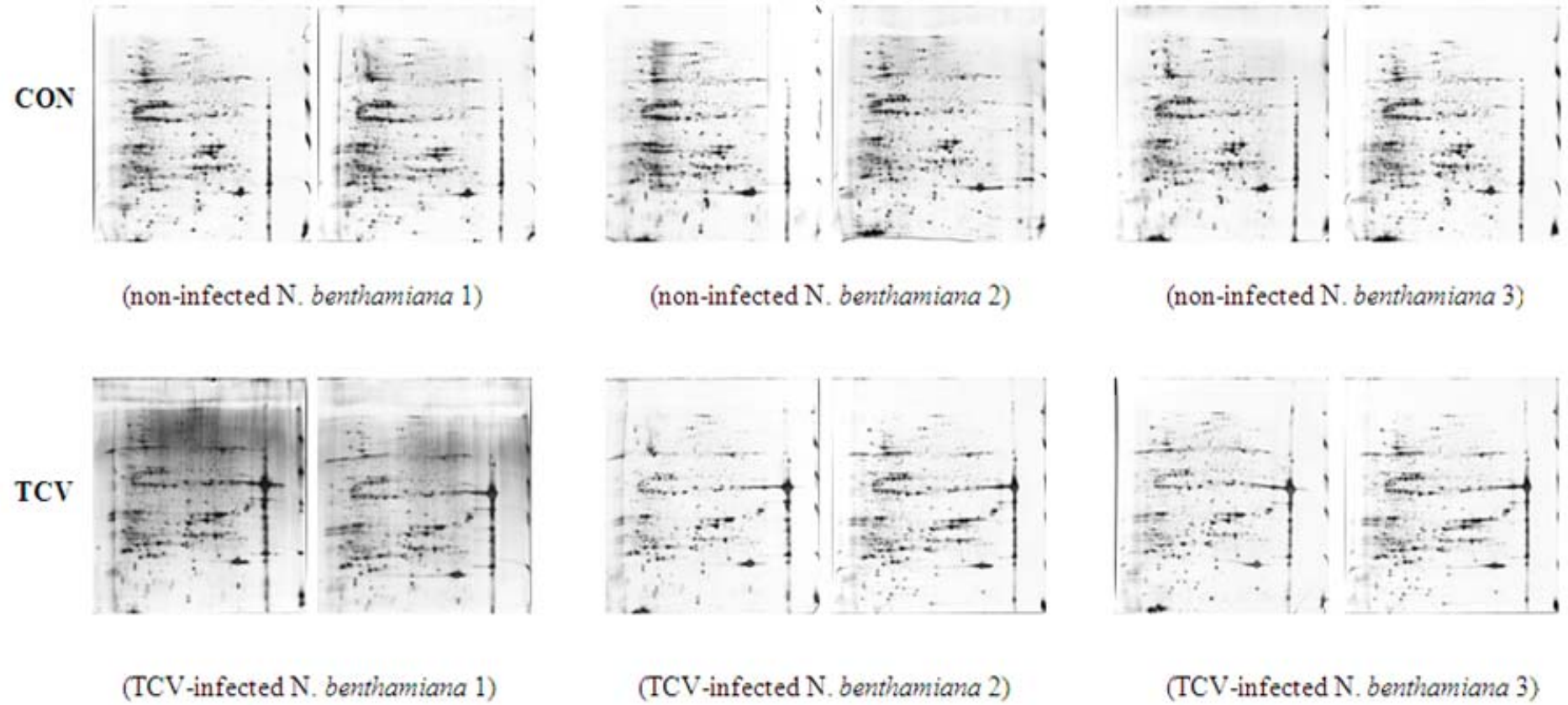


Figure 4.2 2-DE gels of non-infected *N. benthamiana* and TCV-infected *N. benthamiana* leaf protoplast protein. Proteins were extracted from leaf protoplasts and resolved with 2-DE with 18cm pH 3-10NL strips and 12.5% PAGE gels and spots were visualized with silver staining.

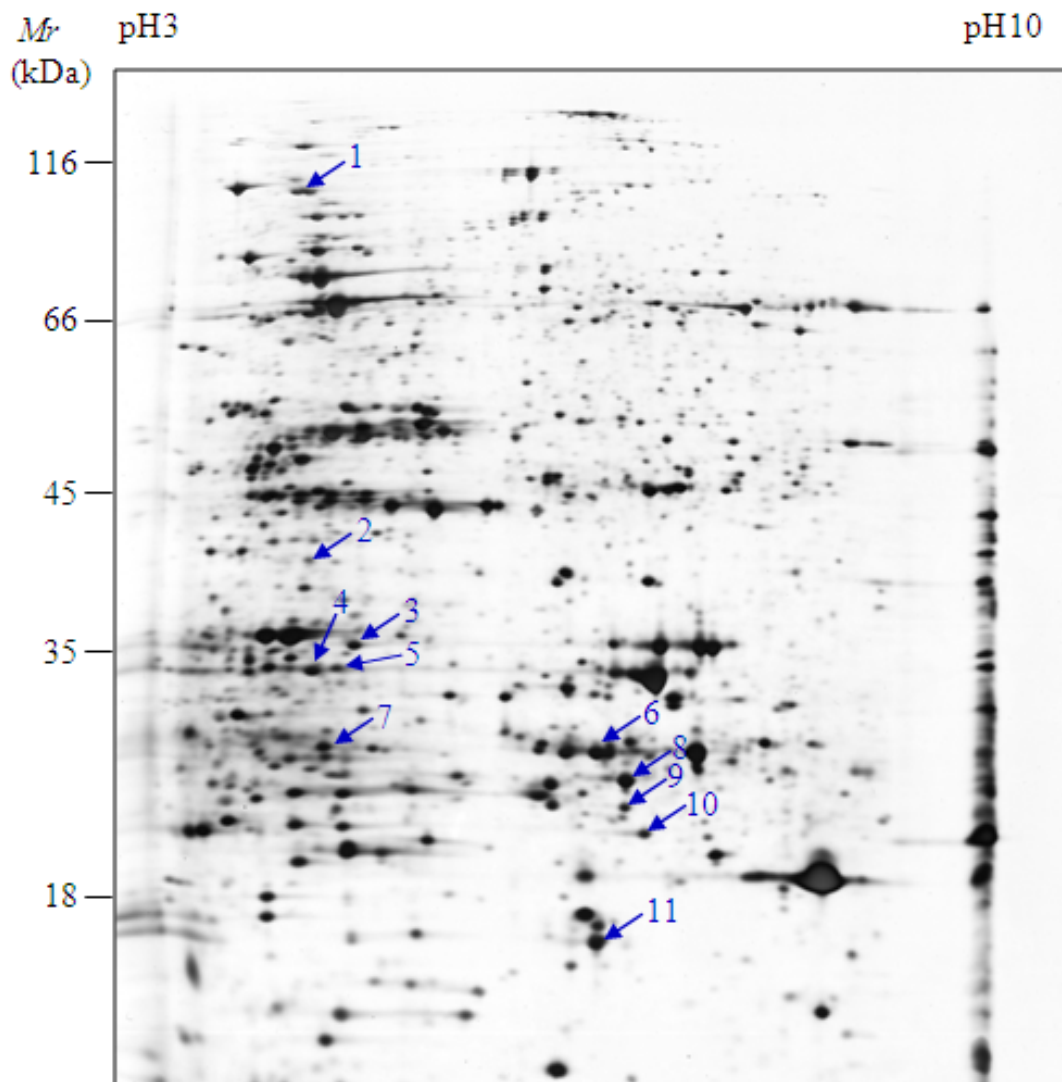


Figure 4.3 A representative 2-DE map of proteins extracted from protoplasts of non-infected *N. benthamiana* leaves and analysis of the proteome profile. Labeled spots represent proteins with significant changes. Spots labeled with blue color showed lower expression in TCV-infected *N. benthamiana*.

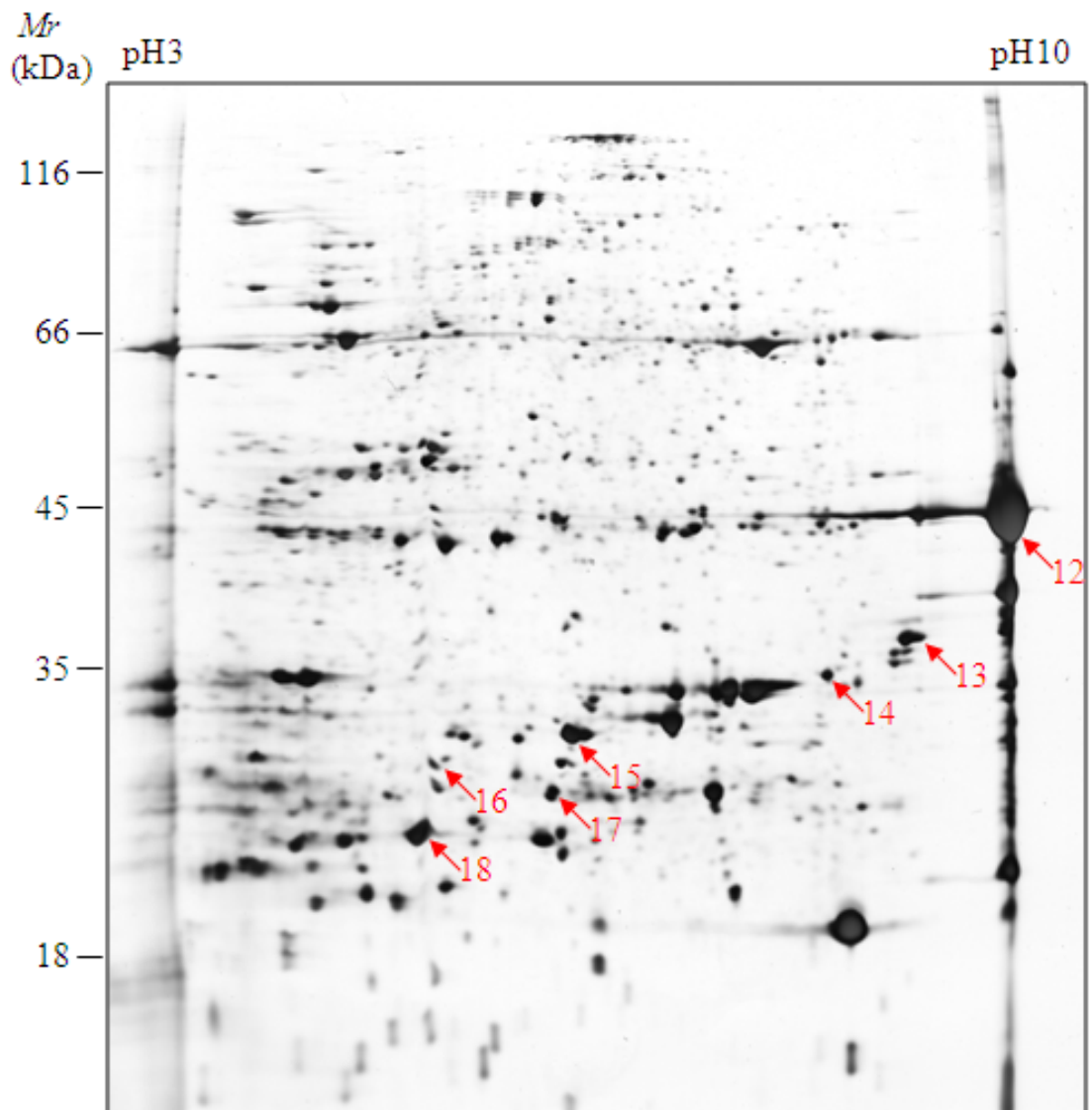


Figure 4.4 A representative 2-DE map of proteins extracted from protoplasts of TCV-infected *N. benthamiana* leaves the analysis of the proteome profile. Labeled spots represent proteins with significant changes. Spots labeled with red showed higher expression in TCV-infected *N. benthamiana*.

4.2.3 Identification of differentially expressed proteins

Among the proteins found with expressions that were significantly different between the two samples, 18 spots were identified. Seven spots (Figures 4.4 and 4.5) with higher expression in TCV-infected *N. benthamiana* were the coat protein of TCV (spots 12-15, 18), L-ascorbate peroxidase (spot 16), triose phosphate isomerase cytosolic isoform-like (spot 17). Eleven spots (Figures 4.3 and 4.5) which showed lower expression in TCV-infected *N. benthamiana* were RuBisCO (spots 6, 8-11), RuBisCO activase 2 (spot 3), RuBisCO activase (spots 4-5), Hsp70 (spot 1), chloroplast carbonic anhydrase (spot 7), ATP synthase CF1 alpha subunit (spot 2). Detailed information of these identified proteins (spot number, protein name, GenInfo Identifier, protein score and searched *pI* and *Mr* are listed in Table 4.1).

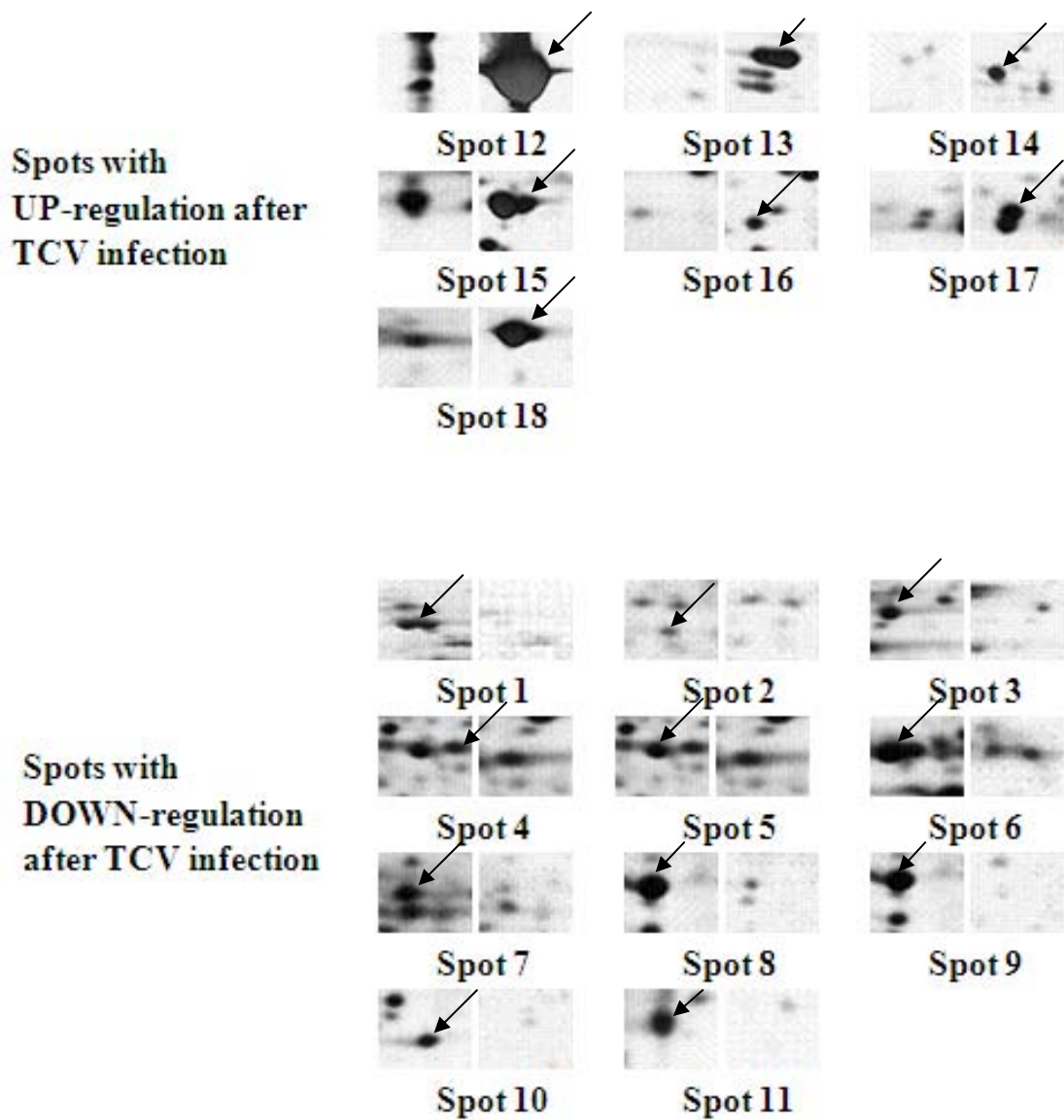


Figure 4.5 Spots with significant change. Spots 1-11 showed lower expression whereas spots 12-18 showed higher expression in TCV-infected *N. benthamiana*,

Table 4.1 Differentially Expressed Proteins between TCV-infected and non-infected *N. benthamiana* protoplast.

Spot no. ¹	Protein name	GenInfo Identifier ²	Protein score ³	Searched <i>pI</i> ⁴	Searched <i>Mr</i> (kDa)
1	hsp70	gi 20559	259	5.07	71
2	ATP synthase CF1 alpha subunit	gi 169794058	150	5.22	56
3	RuBisCO activase 2, chloroplast precursor	gi 12643758	535	8.14	48
4	Ribulose-bisphosphate carboxylase activase	gi 100380	584	5.01	26
5	RuBisCO activase	gi 445628	307	5.50	43
6	RuBisCO large subunit	gi 87204408	343	6.46	50
7	Chloroplast carbonic anhydrase	gi 62865753	233	7.02	21
8	RuBisCO large subunit	gi 13559967	280	6.33	52
9	RuBisCO large subunit	gi 87204408	268	6.46	50
10	RuBisCO large subunit	gi 87204408	268	6.46	50

...CONTINUED

Spot no. ¹	Protein name	GenInfo Identifier ²	Protein score ³	Searched <i>pI</i> ⁴	Searched <i>Mr</i> (kDa)
11	RuBisCO large subunit	gi 87204408	464	6.46	50
12	TCV coat protein	gi 82706242	342	9.31	38
13	TCV coat protein	gi 32263862	321	9.39	38
14	TCV coat protein	gi 32263862	289	9.39	38
15	TCV coat protein	gi 82706242	446	9.31	38
16	L-ascorbate peroxidase	gi 804973	148	5.32	27
17	Triose phosphate isomerase cytosolic isoform-like	gi 77745458	167	5.73	27
18	TCV coat protein	gi 82706242	187	9.31	38

1. Spot numbers are consistent with that presented in **Figure 4.1 and 4.2**. 2. GenInfo Identifier: sequence identification number by GenBank; 3. Protein Score: generated by MS identification platform; a search with protein score over 100 was regarded as a significant match. 4: *pI* and *Mr* are derived from search results generated by the MS platform.

4.3 Discussion

In this study, 2-DE was used to assess the leaf response at protein level in TCV-infected *N. benthamiana* via comparing with the leaf proteome of non-infected *N. benthamiana*. The identified proteins can be categorized into several groups based on their major cellular functions (Table 4.2), such as stress response and detoxification, carbohydrate metabolism and energy metabolism. The major cellular functions of the identified proteins and the cellular processes they are involved in are discussed below:

Stress response and detoxification

Heat shock proteins (HSP) are a class of proteins actively synthesized as part of the response to stress, such as infection, starvation, exposure of the cell to toxins or water deprivation. HSPs are found in virtually all living organisms and also function as intra-cellular chaperones for other proteins. It helps proteins adopt native conformations and correct misfoldings (Sharma & Masison, 2009). HSP 70 can also control virus replication (Santoro, 1994). It was induced by reactive oxygen species (ROS) under stresses (Timperio *et al.*, 2008). The gene expression level of Hsp 70 is up-regulated with phytoplasma infection (Carginale *et al.*, 2004) in *Prunus armeniaca*. However, in this study, Hsp70 (spot 1) was down-regulated in TCV-infected *N. benthamiana* leaves. It is possible that the transcription of Hsp is induced while the translation of Hsp is suppressed by virus. Over-expression of Hsp 70 can increase the cellular resistance to environmental stresses (Kabakov *et al.*, 2006). Therefore, with Hsp 70 down-regulated, the resistance of plants to infection will also decrease

because stresses make the infection easier. If virus suppresses Hsp proteins, the ROS would cause more damages and plants would be more susceptible to virus. So the suppression of Hsp 70 could be one tactic of TCV. Furthermore, Hsp 70 homolog encoded by beet yellows closterovirus functions in cell-to-cell movement of a plant virus (Peremyslov *et al.*, 1999). The mechanism that Hsp increase upon virus infection could be that plant can sense individual properties of particular proteins when expressed at high levels and response to the protein accumulation (Aparicio *et al.*, 2005)

Another spot is identified as L-ascorbate peroxidase (spot 16) which was down-regulated in TCV-infected *N. benthamiana* leaves. Ascorbate peroxidases control the hydrogen peroxide concentration in cells and can attenuate the damaging effects of ROS (Batkova *et al.*, 2008; Dabrowska *et al.*, 2007). It is essential to maintain the antioxidant system and protects plants from stresses (Shigeoka *et al.*, 2001). Ascorbate peroxidase plays an important role in the detoxification of H₂O₂ in higher plants, producing dehydroascorbate and water from H₂O₂ and ascorbate. Its gene expression is induced in a hot pepper that is resistant to one bacterial pathogen (Yoo *et al.*, 2002). Therefore it is possible that virus can suppress ascorbate peroxidase in susceptible plants. In addition, this enzyme helps plants increase tolerance to stresses such as chilling (Kaniuga, 2008) and water stress (Flexas *et al.*, 2006). Since stress and virus infection are close related, the suppression of ascorbate peroxidase can decrease the resistance and make plant further susceptible to virus.

However, study shows that it is inhibited by salicylic acid and 2,6-dichloroisonicotinic acid which are two inducers of plant defense responses (Durner & Klessig, 1995). It is also inhibited by benzothiadiazole which is another inducer of plant defense (Wendehenne *et al.*, 1998). Moreover, cytosolic ascorbate peroxidase is suppressed during pathogen-induced PCD in tobacco (Mittler *et al.*, 1998). On the other hand, ascorbate peroxidase is induced after the onset of necrosis in tobacco (Fodor *et al.*, 1997). Therefore, ascorbate peroxidase is probably differentially regulated during different stages of virus infection.

Carbohydrate Metabolism

As the most abundant protein in leaves, RuBisCO is a key enzyme in the Calvin cycle, it catalyzes the carboxylation (with carbon dioxide) or the oxygenation (with oxygen) of ribulose-1,5-bisphosphate (RuBP). In this study, 5 differential spots were identified as RuBisCO (spots 6, 8-11). RuBisCO activity is affected by various stresses and photosynthetic efficiency can be greatly decreased. Specific transcription factors regulate the differential gene expression (Saibo *et al.*, 2009) of the photosynthesis related genes. Activities of RuBisCO and other Calvin cycle enzymes are also very sensitive to heat stress (Demirevska-Kepova & Feller, 2004). Moreover, the activation state of RuBisCO is suggested as a limiting factor in photosynthesis (Salvucci & Crafts-Brandner, 2004). RuBisCO decreases with the effect of *Albugo candida* in *Arabidopsis thaliana* (Tang *et al.*, 1996). Net photosynthetic rate decreases under the effects of pathogen such as *Thrips tabaci* (Dai *et al.*, 2009). Cucumber

mosaic virus also results in decreased photosynthesis in cucumber and tomato leaves (Song *et al.*, 2009). It showed that photosynthesis would be inhibited by pathogen infection. But not all virus suppress photosynthesis, TMV strain PV42 did not impair photosynthetic acclimation and even enhanced it in some treatments (Balachandran *et al.*, 1994). RuBisCO activity substantially decreases while light reactions are slightly changed in grapevine fan leaf virus-infected tobacco, showing that decreased RuBisCO is the main limitation factor of photosynthesis in virus-infected tobacco (Sampol *et al.*, 2003).

Interestingly, in 2-DE results, only RuBisCO large subunit showed decrease while the small subunit did not show any changes. The RuBisCO holoenzyme is assembled from eight chloroplast-encoded large subunits and eight nuclear-encoded small subunits. Study shows that during oxidative stress, synthesis of large subunit stops and newly synthesized small subunits are rapidly degraded, therefore, assembly of new RuBisCO holoenzyme is inhibited (Knopf & Shapira, 2005). Moreover, the structure of RuBisCO large subunit changes and can not bind the small subunit (Cohen *et al.*, 2005). Excess small subunits would cause the degradation. The different pathways of synthesis are probably responsible for the different responses of large subunit and small subunit.

Triose phosphate isomerase (spot 17) is an important enzyme in glycolysis. It catalyzes the reversible interconversion of the dihydroxyacetone phosphate and D-glyceraldehyde 3-phosphate. Triose phosphate isomerase is down-regulated in rice

mutants which is susceptible to *Magnaporthe oryzae* (Ryu *et al.*, 2009) and up-regulated in some cancer cells (Zhang *et al.*, 2005) and cells under stress (Dihazi *et al.*, 2005). Therefore it is induced under stresses or pathogen infection which is consistent with the 2-DE result that it is up-regulated in TCV-infected *N. benthamiana* leaves. Although triose phosphate isomerase is up-regulated, however, it is not the rate-limiting enzyme in glycolysis. The mechanism whether the up-regulation is due to virus induction or host plant defense is still not clear. Since triose phosphate isomerase is believed to be regulated by abscisic acid in the plant (He & Li, 2008) and abscisic acid is involved in plant defense to pathogens (Mauch-Mani & Mauch, 2005), there should be relationship between virus infection and up-regulation of triose phosphate isomerase.

Table 4.2 Proteins identified with differential expression in *N. benthamiana* protoplasts with TCV infection.

	Proteins that are up-regulated with TCV infection	Proteins that are down-regulated with TCV infection
Virus protein	TCV coat protein (spots 12-15, 18)	-
Stress response and detoxification	L-ascorbate peroxidase (spot 16)	Hsp70 (spot 1)
Carbohydrate Metabolism	Triose phosphate isomerase cytosolic isoform-like (spot 17)	RuBisCO (spots 6, 8-11)
Protein processing	-	RuBisCO activase 2 (spot 3), RuBisCO activase (spots 4-5)
Maintenance of pH	-	Chloroplast carbonic anhydrase (spot 7)
Energy Metabolism	-	ATP synthase CF1 alpha subunit (spot 2)

Protein processing

RuBisCO activase (RCA) is a member of ATPase family and has two isoforms in *N. benthamiana* (Salvucci *et al.*, 1987). It maintains and regulates the activity of RuBisCO. In this study, three spots are identified as RuBisCO activase, one spot is RuBisCO activase 2 (spot 3), the other two spots are RuBisCO activase (spots 4-5) and they are all down-regulated in TCV-infected *N. benthamiana* leaves. RCA responds to stresses such as drought (Demirevska *et al.*, 2008), high temperature (Hendrickson *et al.*, 2007; Salvucci, 2007; Salvucci *et al.*, 2001) and salt stress (Feng *et al.*, 2007). Although there is no previous report about the protein amount change with virus infection, since photosynthesis is affected by virus infection (Bechtold *et al.*, 2005), RuBisCO activase is probably to be suppressed directly or indirectly by the virus.

Maintenance of pH

Chloroplast carbonic anhydrase (Spot 7) is the enzyme that catalyses the reversible hydration of carbon dioxide. Its primary function is to maintain acid-base balance and to transport carbon dioxide. It is affected by salt stress (Siddiqui *et al.*, 2008), aluminum stress (Ali *et al.*, 2008) and cadmium stress (Hayat *et al.*, 2007). With carbonic anhydrase gene silenced, pathogen grew faster in *N. benthamiana* (Restrepo *et al.*, 2005). Therefore its suppression may be caused by virus and can increase the susceptibility of plant to virus. Chloroplast carbonic anhydrase also binds to salicylic acid and plays a role in the hypersensitive defense response (Slaymaker *et*

al., 2002). Therefore the suppression may be also due to the plant resistance response.

Energy Metabolism

ATP synthase CF1 alpha subunit (Spot 2) is the one of many subunits of the catalytic domain (F1 complex) of ATP synthase. ATP synthase is down-regulated under salt stress (Chen *et al.*, 2009), low temperature (Liang *et al.*, 2007) and heat stress (Majoul *et al.*, 2003). It would be damaged by ROS (Lawlor & Tezara, 2009). ATP synthase is up-regulated in virus-resistant shrimp (Zhao *et al.*, 2007) and down-regulated in virus-infected shrimp (Wang *et al.*, 2006). Marek's disease virus phosphorylated polypeptide makes ATP content in mitochondria greatly reduced (Piepenbrink *et al.*, 2009). Therefore it is suppressed by virus infection and the energy metabolism efficiency would also decrease.

Most differentially expressed proteins are related to the carbohydrate metabolism and photosynthesis (Table 4.2). Five down-regulated spots in TCV-infected *N. benthamiana* leaf protein were identified as RuBisCO. Moreover, the RuBisCO activase, which regulates the RuBisCO activity, is also down-regulated with virus infection. RCA relies on ATP to activate the RuBisCO, but with the down-regulation of ATP synthase, RCA cannot obtain sufficient ATP to complete the activation of RuBisCO. Therefore, with lower amount and decreased activity of RCA, the activity of RuBisCO would decrease. Furthermore, with less RuBisCO and lower activity, the photosynthesis efficiency would become lower in the TCV-infected *N. benthamiana* than in the healthy *N. benthamiana*.

Besides, ROS, which increases under stress, will cause significant damage to cell structures. Three identified differential proteins; HSP 70, ascorbate peroxidase and ATP synthase are related to ROS. For example, ascorbate peroxidase, which is essential to the detoxification of H_2O_2 , can attenuate the effects of ROS. With decreased expression of ascorbate peroxidase, ROS may cause severe damage to the cells.

Some identified proteins are known to be regulated by hormones, such as triose phosphate isomerase and RuBisCO activase. Many hormones are related to the plant-pathogen interaction (Kazan & Manners, 2009; Kovac *et al.*, 2009; Robert-Seilaniantz *et al.*, 2007). Hormones can trigger some signal transduction pathways (Robert-Seilaniantz *et al.*, 2007), but the underlying mechanism is not clear.

Carbohydrate metabolism is not only related to energy metabolism, it also influences symptom development in virus-infected *Arabidopsis thaliana* (Handford & Carr, 2007). Plant is a whole organism and the pathways are related to each other. In healthy plants, homeostasis is kept and when virus infects, the intruder would trigger many pathways (Figure 4.6). Virus infection triggers signal transduction first and increased ROS production will affect cell homeostasis and cause stresses and generate some toxins. Therefore plant has stress responses, and the toxins have to be detoxified. ROS also causes programmed cell death (PCD), which can prevent the virus spread. The stresses, toxins and PCD all can suppress carbohydrate metabolism and photosynthesis. The suppressed energy metabolism will stimulate more PCD. To

summarize, the pathways in the plants are so complicated and closely related that virus infection affects most of them. Plant adjusts its physiology to keep the homeostasis and virus utilizes plant to express what it needs. The interaction between them also evolved during the evolution of the plant and the virus themselves.

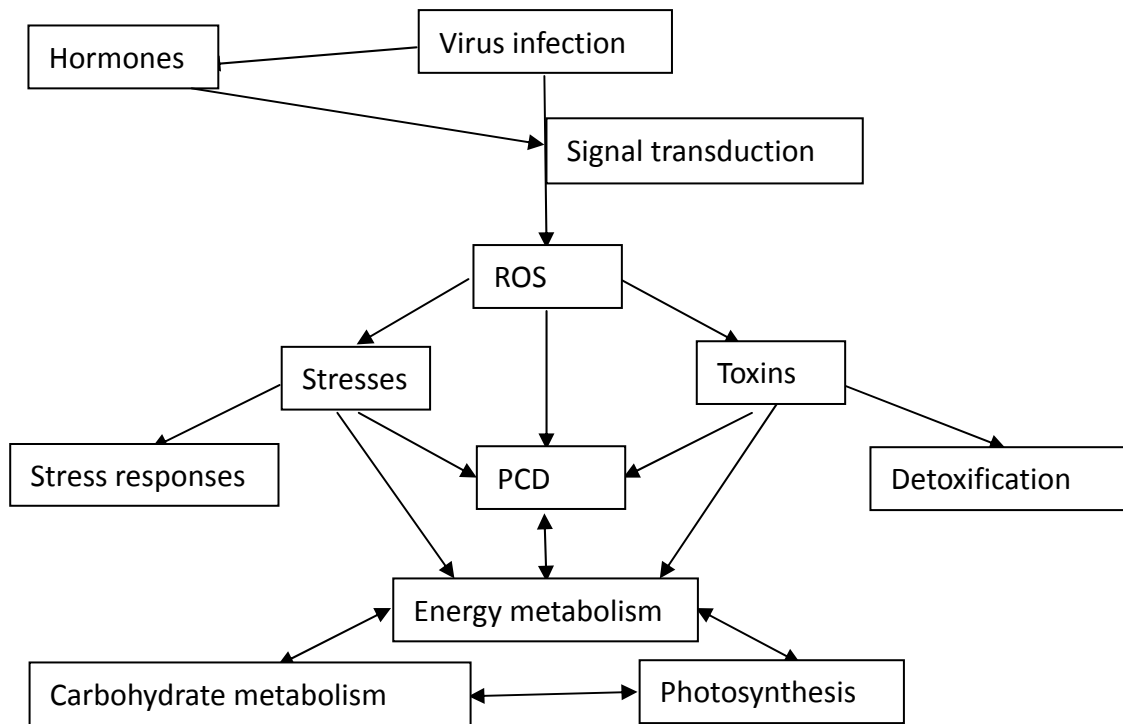


Figure 4.6 The pathways that virus affects in plant.

CHAPTER 5. 2-DE OF PROTEINS EXTRACTED FROM CHLOROPLASTS OF NON-INFECTED VERSUS TCV-INFECTED *NICOTIANA BENTHAMIANA* LEAVES

5.1 Introduction

Chloroplasts conduct photosynthesis by converting solar energy and carbon dioxide to oxygen and sugar. Its functions are regulated by many environmental stresses and virus infections. As an example, virus infection will disrupt chloroplasts (Zhou *et al.*, 2008) and block transport pathways from the chloroplast to the cytosol (Loebenstein, 2006). Cucumber mosaic virus alters the ultrastructure of chloroplasts (Chen *et al.*, 2007). Peach latent mosaic viroid can even inhibit chloroplast development in the early stage (Rodio *et al.*, 2007).

As shown in the 2-DE of TCV-infected and non-infected *N. benthamiana* protoplasts, virus infection down-regulated the RuBisCO and RuBisCO activase. These two enzymes are key enzymes in the Calvin cycle. In other words, the functions of chloroplasts are affected. However, the interactions between the chloroplasts and the TCV-infected plants are still not clear. To investigate which proteins are affected in chloroplasts and how chloroplasts react to the TCV infection, 2-DE of proteins from non-infected and TCV-infected *N. benthamiana* chloroplasts was performed. After that, comprehensive analyses of proteins associated with TCV infection were focused on the differently expressed proteins.

5.2 Results

5.2.1 Extraction of total proteins from chloroplasts

Proteins of TCV-infected and non-infected *N. benthamiana* chloroplasts were extracted using protocols as mentioned in Chapter 2. Then the protein assay was used to determine the concentration of the protein samples. The protein amount and concentration were calculated according to the standard curve (Figure 5.1).

5.2.2 2-DE of chloroplast proteins and protein expression profile

Three biological replicates were performed and 2-DE was optimized to better separate the proteins and Proteins (20 µg) were first loaded onto a pH 4-7 IPG strip for the first dimensional separation followed by 12.5% SDS-PAGE for the second dimensional separation. The gels were then stained with silver nitrate to reveal the protein spots (Figures 5.2 and 5.3). The developing time was 2 min.

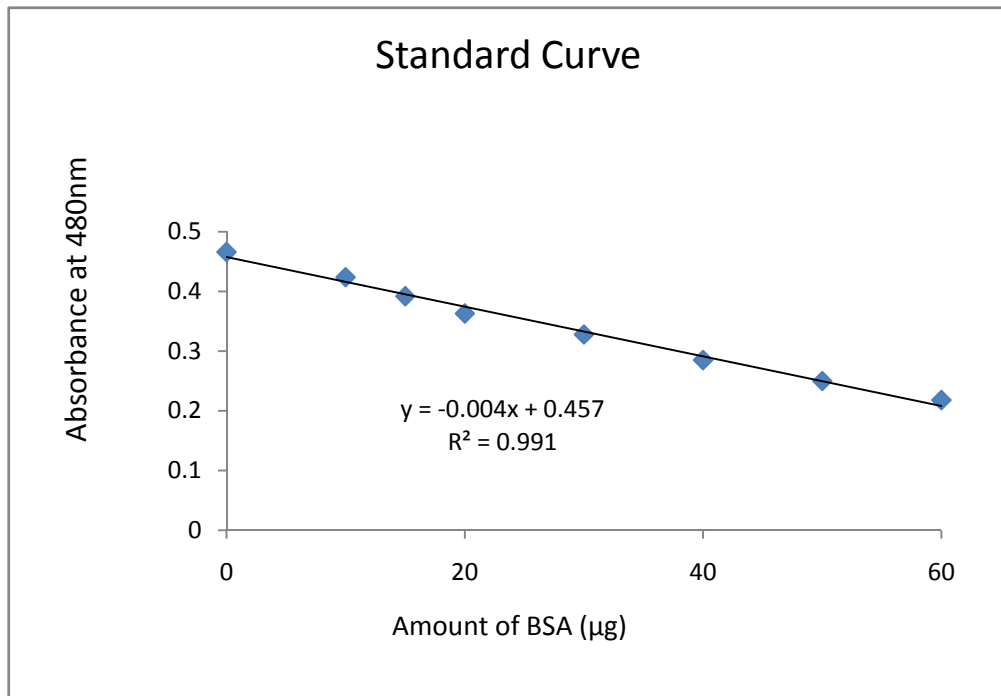


Figure 5.1 Standard curve of the protein quantification assay.

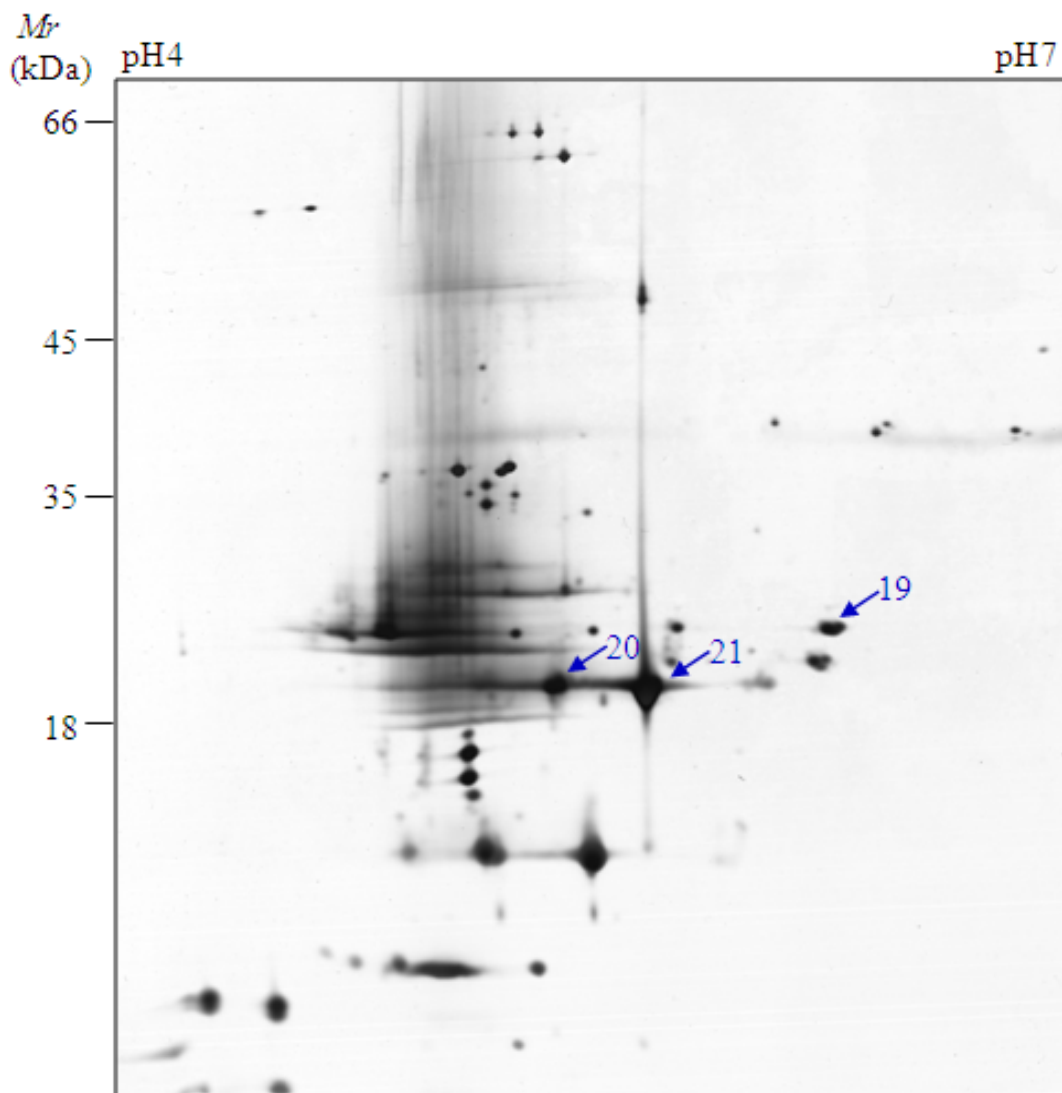


Figure 5.2 A representative 2-DE map of proteins from chloroplasts of non-infected *N. benthamiana* and the analysis of the proteome profile. Spots labeled with blue color showed lower expression in TCV-infected *N. benthamiana* compared with those in non-infected *N. benthamiana*.

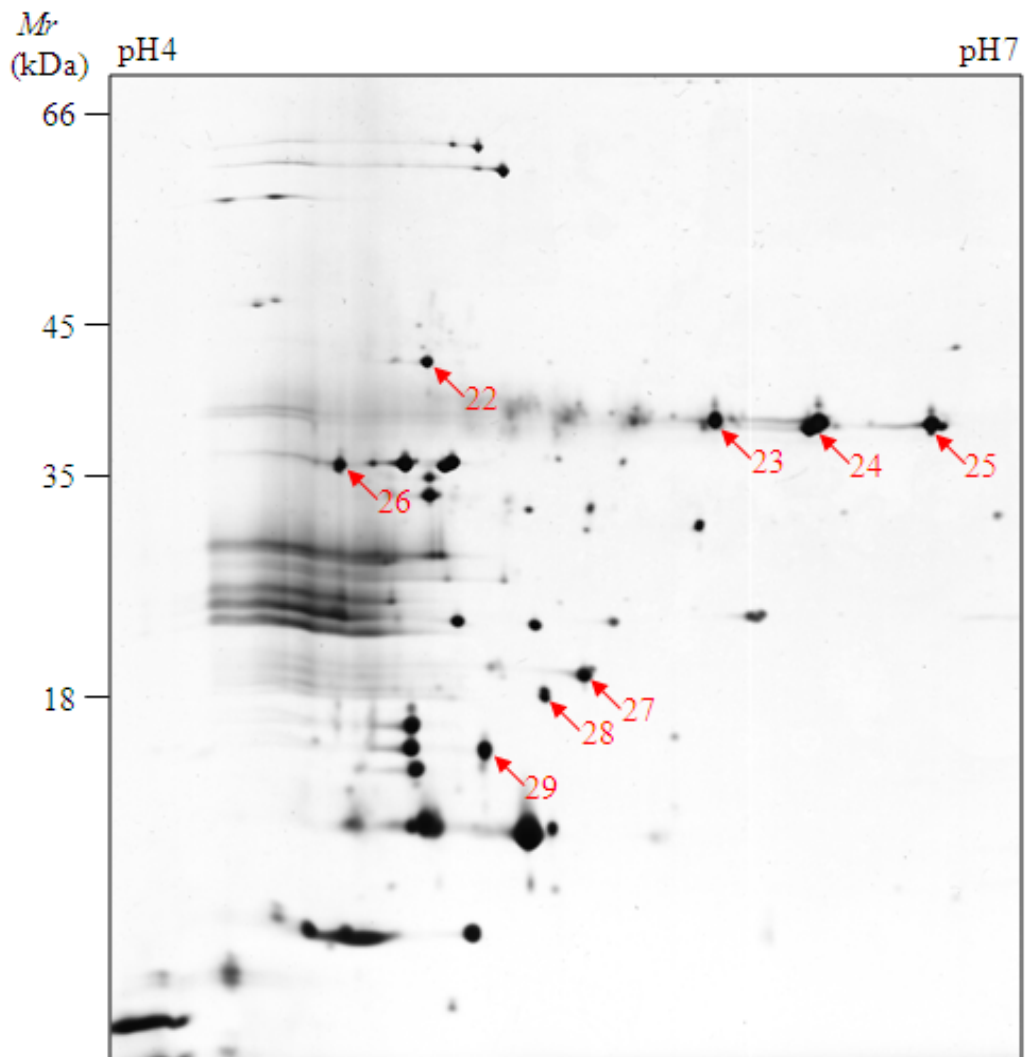


Figure 5.3 A representative 2-DE map of proteins from chloroplasts of TCV-infected *N. benthamiana* and the analysis of the proteome profile. Spots labeled with red color showed higher expression in TCV-infected *N. benthamiana* compared with those in non-infected *N. benthamiana*.

5.2.3 Identification of differentially expressed proteins in the chloroplast

Eleven spots with significant changes were identified. Eight spots with higher expression in TCV-infected *N. benthamiana* were putative zinc protease (spot 22), hypothetical protein Anaek_0416 (Spot 26), Ferredoxin--NADP reductase (spots 23-25), photosystem I light-harvesting chlorophyll a/b-binding protein (spot 27), 23-kDa polypeptide of photosystem II oxygen-evolving complex (spot 28) and fkbp-type peptidyl-prolyl cis-trans isomerase 2 (spot 29). Three spots which showed lower expression in TCV-infected *N. benthamiana* were identified as well; they were Chlorophyll A-B binding protein (spots 20 and 21) and adenylate kinase (spot 19). Detailed information of these identified proteins (spot number, protein name, GenInfo Identifier, protein score and searched *pI* and *Mr*) are listed in Table 5.1.

5.3 Discussion

The identified proteins can be categorized into several groups based on their major cellular functions, such as Protein degradation, Photosynthesis and energy metabolism (Table 5.2). The major cellular functions of the identified proteins and the cellular processes they are involved in are discussed below:

Table 5.1 Differentially Expressed Proteins between TCV-infected and non-infected *N. benthamiana* chloroplast proteins.

Spot no.¹	Protein name	GenInfo Identifier²	Protein score³	Searched <i>pI</i>⁴	Searched <i>Mr</i> (kDa)
19	Adenylate kinase	gi 225355115	53	5.19	23
20	Chlorophyll A-B binding protein	gi 7271945	174	5.59	18
21	Chlorophyll A-B binding protein	gi 7271945	160	5.59	18
22	Putative zinc protease	gi 27734210	62	5.65	49
23	Ferredoxin--NADP reductase	gi 3913651	139	8.37	40
24	Ferredoxin--NADP reductase	gi 3913651	244	8.37	40
25	Ferredoxin--NADP reductase	gi 3913651	192	8.37	40

...CONTINUED

Spot no. ¹	Protein name	GenInfo Identifier ²	Protein score ³	Searched <i>pI</i> ⁴	Searched <i>Mr</i> (kDa)
26	Hypothetical protein Anaek_0416	gi 197120836	62	4.73	10
27	Photosystem I light-harvesting chlorophyll a/b-binding protein	gi 493723	71	5.83	26
28	RNA polymerase sigma-70 factor	gi 84515072	61	9.21	24
29	fkbp-type peptidyl-prolyl cis-trans isomerase 2	gi 223530783	91	9.28	24

1. Spot numbers are consistent with those presented in **Figures 5.3 and 5.4**. 2. GenInfo Identifier: sequence identification number by GenBank; 3. Protein Score: generated by MS identification platform; a search with protein score over 50 was regarded as a significant match. 4: *pI* and *Mr* are derived from search results generated by the MS platform.

Protein degradation

Virus infection is closely related to protein metabolism. A model that virus can reorganize the ER and increase protein degradation was proposed previously (Ju *et al.*, 2005). Microarray analysis also showed that virus infection affected protein degradation in Arabidopsis (Marathe *et al.*, 2004). On the other hand, increase in the protein degradation may also be the one of many resistance strategies for the plants to fight against the virus (Martin *et al.*, 2003). Zinc protease (spot 22) is a metalloproteases and participates in proteolysis. Some zinc proteases have roles in cell signaling (Shih *et al.*, 2008). This is the first time to have this protein identified in virus-infected plant proteome. Although there is no data about this protein in virus-infected plant, other proteases are proved to take part in host-virus interaction. Plant vacuolar protease mediates virus-induced hypersensitive cell death (Hatsugai *et al.*, 2004). A plasminogen-activating protease even controls the development of primary pneumonic plague (Lathem *et al.*, 2007). Virus infection may trigger cell signaling pathways and increase the protein degradation.

Protein processing

Peptidyl-prolyl cis-trans isomerase is a family of enzymes. It catalyzes the cis-trans isomerization of proline imidic peptide bonds in oligopeptides and accelerates the folding of proteins. It is related to oxidative stress (Hong *et al.*, 2002) and may also take part in other stress responses. Although the response pathway can not be deduced, at least we can know that protein processing is related to the virus

infection.

Photosynthesis

There are two differentially expressed enzymes related to photosynthesis: ferredoxin-NADP reductase (Spots 23-25) and chlorophyll a/b-binding protein (spots 20 and 21). Ferredoxin-NADP reductase belongs to the family of oxidoreductases and catalyzes the oxidation of ferredoxin. Chloroplast ferredoxin plays an important role in plant cells by participating in many pathways. Environmental stresses cause the ferredoxin decline (Tognetti *et al.*, 2007) and the ferredoxin-NADP reductase is possible to increase as a response to the ferredoxin starvation. It is also the first time to detect ferredoxin-NADP reductase as a differentially expressed protein in virus-infected plant.

Chlorophyll a/b-binding protein balances the excitation energy between photosystems I and II. Its gene expression changes in response to drought and saline habitats (Wang *et al.*, 1998), and also to the light stress (Potter *et al.*, 1996). However, chlorophyll analysis suggests that the suppression of light reactions is a minor effect of virus infection (Sampol *et al.*, 2003). It is possible because the change of chlorophyll a/b-binding protein could not be detected on the 2-DE gels of total protoplast proteins, but the difference appeared on the gels of chloroplast proteins of which chlorophyll a/b-binding protein is much more enriched. Although there is no evidence that it is related to virus infection, the stresses caused by virus may also affect the chlorophyll a/b-binding protein.

Transcription

RNA polymerase is an essential enzyme and controls the transcription. After infection, virus needs to synthesize its own proteins and RNA, so the transcription level will increase. Some antiviral proteins mainly inhibit virus transcription (Habjan *et al.*, 2009). In chloroplasts, photosynthesis is suppressed by virus and RuBisCO is down-regulated, therefore, as a response, the transcription level is possible to increase to make up the decrease in the photosynthesis enzymes.

Energy Metabolism

Adenylate kinase controls the interconversion between ADP and ATP, so it is a key enzyme in energy metabolism. It regulates multiple intracellular and extracellular energy-dependent and nucleotide signaling processes, so it is very sensitive in stress response (Dzeja & Terzic, 2009). Hepatitis C virus RNA helicase consists of three structural domains and two of them have an adenylate kinase like fold, including a phosphate-binding loop in the first domain (Kim *et al.*, 1998).

The pathways to which these proteins belong are also closely related in chloroplasts. First, photosynthesis generates energy from light, and then adenylate kinase provides energy supply. Transcription and protein degradation keep the homeostasis. When virus infects the plant and enters chloroplasts, photosynthesis is suppressed so energy supply is not enough. Transcription level is up-regulated by plant to make up the decrease in photosynthesis or by virus to transcribe the host genes which are useful to virus. After virus triggers ROS and PCD by signal

transduction cascades, protein degradation is up-regulated. If plant can recognize virus protein, protein degradation would also be activated.

Among proteins identified above, several lack the information about plant-virus interaction. One reason is that plant material is *N. benthamiana* that does not have full genome information in databases. Proteins have to be identified by homolog alignment. The other reason is that chloroplast is seldom studied separately in proteomic analysis. 2-DE results showed the effectiveness of the method we use. More differentially expressed proteins can be identified and with the information of compartment alization, the mechanisms of biological processes can be further understood.

To sum up, virus infection affects many pathways such as protein degradation, photosynthesis and energy metabolism in chloroplasts. Plants also respond to the infection and trigger more pathways. The mechanism is still not clear because the relationship between the host and virus may be very complicated.

Table 5.2 Proteins identified with differential expression in *N. benthamiana* with TCV infection.

	Proteins that are up-regulated with TCV infection	Proteins that are down-regulated with TCV infection
Protein degradation	zinc protease (spot 22)	-
Protein processing	fkbp-type peptidyl-prolyl cis-trans isomerase 2 (spot 29)	-
Photosynthesis	Ferredoxin--NADP reductase (spots 23-25), Chlorophyll a/b-binding protein (spot 27)	Chlorophyll a/b binding protein (spots 20-21)
Transcription	RNA polymerase sigma-70 factor (spot 28)	-
Energy Metabolism	-	Adenylate kinase(Spot 19)

CHAPTER 6. REAL-TIME PCR OF DOWN-REGULATED RUBISCO GENE IN NON-INFECTED VERSUS TCV-INFECTED *NICOTIANA BENTHAMIANA* LEAVES

6.1 Introduction

Real-time PCR was first developed by Higuchi (Higuchi *et al.*, 1993) and has several advantages. As a rapid and sensitive technique to reveal the RNA level, it is also widely used in plant gene expression investigations (Aime *et al.*, 2008; Desmond *et al.*, 2008).

During evolution, plants have developed some kinds of defense mechanisms to respond to viral infection (Lu *et al.*, 2008; Qu & Morris, 2005). For example, if pathogen was recognized by the plant and the resistance (R) gene was triggered, hypersensitive response will take place (Gan *et al.*, 2009; Kamoun *et al.*, 1999). It induces PCD (Hofius *et al.*, 2007; Khurana *et al.*, 2005), activates several signal transduction pathways (Rathjen & Moffett, 2003; Romero-Puertas *et al.*, 2004) and causes necrotic local lesions to avoid systematic infection (Kuta & Tripathi, 2005).

RuBisCO, the most abundant protein in the leaves, also catalyzes the key enzyme in the Calvin cycle. It is highly conserve among plants. In the 2-DE mentioned above, 5 spots were identified as RuBisCO's large subunit. The expression was down-regulated at the protein level, but the change at transcription level is still unknown. Some transcription factors are known to regulate the gene expression of the photosynthesis related genes (Saibo *et al.*, 2009).

In this Chapter, RNA from non-infected *N. benthamiana* and TCV-infected *N. benthamiana* was extracted and cDNA was generated from the RNA. Real-time PCR was performed to compare the transcription level of RuBisCO large subunit gene.

6.2 Results

6.2.1 Synthesis of the Real-time PCR primers of RuBisCO large subunit gene

Total RNA was extracted and reverse-transcribed as described in Chapter 2. Since RuBisCO large subunit gene is highly conserve among plants, the real-time PCR primer from rice (Yan *et al.*, 2006) was tried on *N. benthamiana* cDNA. After PCR reaction, there was an apparent band around 0.6 kb and this band was excised from agarose gel and purified for DNA sequencing. The sequencing result showed that it was a RuBisCO large subunit gene fragment.

Primers for RuBisCO large subunit:

Forward primer: 5'-GCAGGTACATGCGAAGAAATG-3'

Reverse primer: 5'-TCACAAGCTGCGGCTAGTTC-3'

Primers for *N. benthamiana* actin:

Forward primer: 5'-CTTGAAACAGCAAAGACCAGC-3'

Reverse primer: 5'-GGAATCTCTCAGCACCAATGG-3'

6.2.2 Real-time PCR of RuBisCO large subunit

Total RNA was extracted from non-infected *N. benthamiana* and TCV-infected *N. benthamiana* leaves. The cDNA was generated by reverse transcription as mentioned above. Real-time PCR was performed in triplicate and the fold change was calculated

based on the Ct values (Tables 6.1 & 6.2). All data were normalized to *N. benthamiana* actin expression levels as previously described (Livak & Schmittgen, 2001). To normalize the RT-PCR, one endogenous reference gene (actin) was used in each experiment. Results were expressed as a threshold cycle (Ct) value. Each RNA sample was assayed in triplicate and their Ct and standard deviation values were averaged. The RuBisCO large subunit expression showed a decrease by 62% in *N. benthamiana* with TCV infection (Figure 6.1).

6.3 Discussion

The RuBisCO large subunit gene expression was largely down-regulated in TCV-infected *N. benthamiana* (Figure 6.1). This is consistent with the 2-DE results in which 5 spots were down-regulated in TCV-infected *N. benthamiana* and identified as RuBisCO large subunit. Therefore, the virus infection affects the RuBisCO expression beginning from the transcription level. Many other signal transduction pathways may also be affected.

RuBisCO is a key enzyme in the Calvin cycle and plants cannot utilize the carbon dioxide without it. Therefore, although TCV suppresses its transcription, the expression cannot be shut down, or else the plant cannot live and the virus will not be able to replicate. On the other hand, plant also develops PCD and causes necrotic local lesions to avoid systematic infection (Kuta & Tripathi, 2005).

Table 6.1 Ct value of the Real-time PCR.

Sample	Non-infected <i>N. benthamiana</i>			TCV-infected <i>N. benthamiana</i>		
	1	2	3	1	2	3
Actin	20.34	21.07	19.43	20.97	22.05	20.46
RuBisCO large subunit	24.88	25.63	24.86	26.68	28.5	27.02
Δ Ct	4.54	4.56	5.43	5.71	6.45	6.56

Table 6.2 Comparison of RuBisCO large subunit gene expression in TCV-infected *N. benthamiana* with non-infected *N. benthamiana*.

	Non-infected <i>N. benthamiana</i>	TCV-infected <i>N. benthamiana</i>
Δ Ct	4.84	6.24
s	0.51	0.46
$\Delta \Delta$ Ct	1.4	
$2^{-\Delta \Delta \text{Ct}}$	0.38	

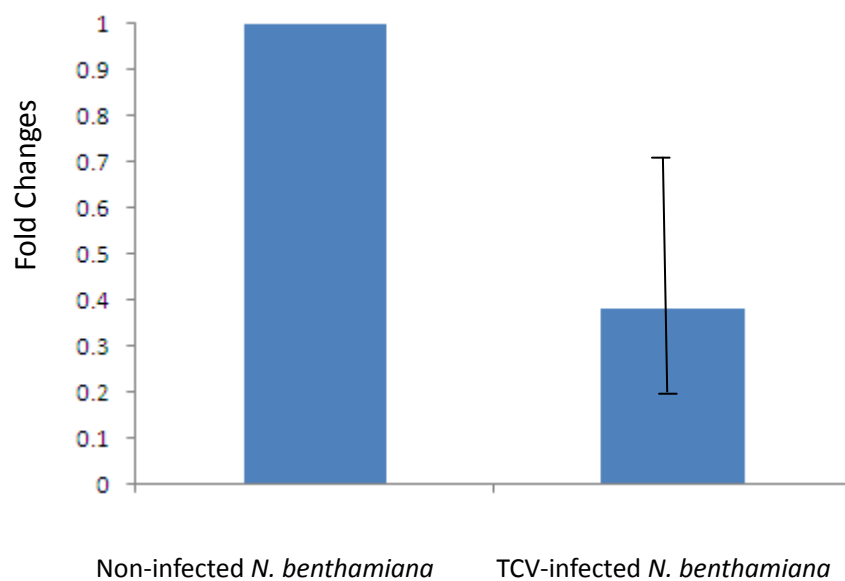


Figure 6.1 Comparison of RuBisCO large subunit gene expressions in non-infected versus TCV-infected *N. benthamiana*. RuBisCO large subunit gene showed apparent down-regulation in TCV-infected *N. benthamiana*.

Interestingly, the other component of RuBisCO protein, the small subunit, did not

show great down-regulation in the 2-DE analysis. It is possible that the amount of RuBisCO is mainly regulated by the large subunit, or the virus affects more on the large subunit gene expression than on the small subunit.

Plant-pathogen interaction makes a balance between them so that virus can stay in the plant for a long time. It is very complicated and many pathways are involved in the relationship. Furthermore, with evolution more efficient ways will be developed by both the host and the pathogen.

Literature cited

Aime S, Cordier C, Alabouvette C, Olivain C (2008) Comparative analysis of PR gene expression in tomato inoculated with virulent *Fusarium oxysporum* f. sp. *lycopersici* and the biocontrol strain *F. oxysporum* Fo47. *Physiological and Molecular Plant Pathology* **73**: 9-15

Ali B, Hasan SA, Hayat S, Hayat Q, Yadav S, Fariduddin Q, Ahmad A (2008) A role for brassinosteroids in the amelioration of aluminium stress through antioxidant system in mung bean (*Vigna radiata* L. Wilczek). *Environmental and Experimental Botany* **62**: 153-159

Aparicio F, Thomas CL, Lederer C, Niu Y, Wang DW, Maule AJ (2005) Virus induction of heat shock protein 70 reflects a general response to protein accumulation in the plant cytosol. *Plant Physiology* **138**: 529-536

Balachandran S, Osmond CB, Makino A (1994) Effects of 2 strains of tobacco mosaic-virus on photosynthetic characteristics and nitrogen partitioning in leaves of *nicotiana-tabacum* cv *xanthi* during photoacclimation under 2 nitrogen nutrition regimes. *Plant Physiology* **104**: 1043-1050

Batkova P, Pospisilova J, Synkova H (2008) Production of reactive oxygen species and development of antioxidative systems during in vitro growth and ex vitro transfer. *Biologia Plantarum* **52**: 413-422

Bechtold U, Karpinski S, Mullineaux PM (2005) The influence of the light environment and photosynthesis on oxidative signalling responses in plant-birotrophic pathogen interactions. *Plant Cell and Environment* **28**: 1046-1055

Berggard T, Linse S, James P, Bt (2007) Methods for the detection and analysis of protein-protein interactions. *Proteomics* **7**: 2833-2842

Biemann K (1988) Contributions of mass-spectrometry to peptide and protein-structure. *Biomedical and Environmental Mass Spectrometry* **16**: 99-111

Bjellqvist B, Basse B, Olsen E, Celis JE (1994) Reference points for comparisons of 2-dimensional maps of proteins from different human cell-types defined in a pH scale where isoelectric points correlate with polypeptide compositions. *Electrophoresis* **15**: 529-539

Breitling R, Pitt AR, Barrett MP (2006) Precision mapping of the metabolome. *Trends in Biotechnology* **24**: 543-548

- Bustin SA (2000) Absolute quantification of mRNA using real-time reverse transcription polymerase chain reaction assays. *Journal of Molecular Endocrinology* **25**: 169-193
- Canovas FM, Dumas-Gaudot E, Recorbet G, Jorin J, Mock HP, Rossignol M (2004) Plant proteome analysis. *Proteomics* **4**: 285-298
- Carginale V, Maria G, Capasso C, Ionata E, La Cara F, Pastore M, Bertaccini A, Capasso A (2004) Identification of genes expressed in response to phytoplasma infection in leaves of *Prunus armeniaca* by messenger RNA differential display. *Gene* **332**: 29-34
- Carrington JC, Heaton LA, Zuidema D, Hillman BI, Morris TJ (1989) The genome structure of turnip crinkle virus. *Virology* **170**: 219-226
- Carrington JC, Morris TJ, Stockley PG, Harrison SC (1987) Structure and assembly of turnip crinkle virus .4. analysis of the coat protein gene and implications of the subunit primary structure. *Journal of Molecular Biology* **194**: 265-276
- Chen FF, Du ZY, Liu X, Xie L, Chen JS (2007) Effect of cucumber mosaic virus-encoded 2b protein on photosynthesis and chloroplast structure of the host plant. *Progress in Biochemistry and Biophysics* **34**: 889-896
- Chen SX, Harmon AC (2006) Advances in plant proteomics. *Proteomics* **6**: 5504-5516
- Chen X, Wang Y, Li JY, Jiang AL, Cheng YW, Zhang W (2009) Mitochondrial proteome during salt stress-induced programmed cell death in rice. *Plant Physiology and Biochemistry* **47**: 407-415
- Cocking E (1960) A Method for the Isolation of Plant Protoplasts and Vacuoles. *Nature* **187**: 962-963
- Cohen I, Knopf JA, Irihimovitch V, Shapira M (2005) A proposed mechanism for the inhibitory effects of oxidative stress on rubisco assembly and its subunit expression. *Plant Physiology* **137**: 738-746
- Cohen Y, Qu F, Gisel A, Morris TJ, Zambryski PC (2000) Nuclear localization of turnip crinkle virus movement protein p8. *Virology* **273**: 276-285
- Corneau J, Barthou H, Jauneau A, Petitprez M, Pont-Lezica R, Galaud JP (2002)

Cellular import of synthetic peptide using a cell-permeable sequence in plant protoplasts. *Plant Physiology and Biochemistry* **40**: 1081-1086

Dabrowska G, Katai A, Goc A, Szechynska-Hebda M, Skrzypek E (2007) Characteristics of the plant ascorbate peroxidase family. *Acta Biologica Cracoviensia Series Botanica* **49**: 7-17

Dai YJ, Shao MM, Hannaway D, Wang LL, Liang JP, Hu L, Lu H (2009) Effect of Thrips tabaci on anatomical features, photosynthetic characteristics and chlorophyll fluorescence of Hypericum sampsonii leaves. *Crop Protection* **28**: 327-332

Davey MR, Anthony P, Power JB, Lowe KC (2005) Plant protoplasts: status and biotechnological perspectives. *Biotechnology Advances* **23**: 131-171

Demirevska K, Simova-Stoilova L, Vassileva V, Feller U (2008) Rubisco and some chaperone protein responses to water stress and rewatering at early seedling growth of drought sensitive and tolerant wheat varieties. *Plant Growth Regulation* **56**: 97-106

Demirevska-Kepova K, Feller U (2004) Heat sensitivity of Rubisco, Rubisco activase and Rubisco binding protein in higher plants. *Acta Physiologiae Plantarum* **26**: 103-114

Desmond OJ, Manners JM, Schenk PM, Maclean DJ, Kazan K (2008) Gene expression analysis of the wheat response to infection by Fusarium pseudograminearum. *Physiological and Molecular Plant Pathology* **73**: 40-47

Dihazi H, Asif AR, Agarwal NK, Doncheva Y, Muller GA (2005) Proteomic analysis of cellular response to osmotic stress in thick ascending limb of Henle's loop (TALH) cells. *Molecular & Cellular Proteomics* **4**: 1445-1458

Durner J, Klessig DF (1995) Inhibition of ascorbate peroxidase by salicylic-acid and 2,6-dichloroisonicotinic acid, 2 inducers of plant defense responses. *Proceedings of the National Academy of Sciences of the United States of America* **92**: 11312-11316

Dzeja P, Terzic A (2009) Adenylate Kinase and AMP Signaling Networks: Metabolic Monitoring, Signal Communication and Body Energy Sensing. *International Journal of Molecular Sciences* **10**: 1729-1772

Feng LL, Han YJ, Liu G, An BG, Yang J, Yang GH, Li YS, Zhu YG (2007) Overexpression of sedoheptulose-1,7-bisphosphatase enhances photosynthesis and growth under salt stress in transgenic rice plants. *Functional Plant Biology* **34**: 822-834

Fenn JB, Mann M, Meng CK, Wong SF, Whitehouse CM (1989) Electrospray ionization for mass-spectrometry of large biomolecules. *Science* **246**: 64-71

Flexas J, Bota J, Galmes J, Medrano H, Ribas-Carbo M (2006) Keeping a positive carbon balance under adverse conditions: responses of photosynthesis and respiration to water stress. *Physiologia Plantarum* **127**: 343-352

Fodor J, Gullner G, Adam AL, Barna B, Komives T, Kiraly Z (1997) Local and systemic responses of antioxidants to tobacco mosaic virus infection and to salicylic acid in tobacco - Role in systemic acquired resistance. *Plant Physiology* **114**: 1443-1451

Gan YZ, Zhang LS, Zhang ZG, Dong SM, Li J, Wang YC, Zheng XB (2009) The LCB2 subunit of the sphingolip biosynthesis enzyme serine palmitoyltransferase can function as an attenuator of the hypersensitive response and Bax-induced cell death. *New Phytologist* **181**: 127-146

Geisow MJ (1998) Proteomics: One small step for a digital computer, one giant leap for humankind. *Nature Biotechnology* **16**: 206-206

Gorg A, Obermaier C, Boguth G, Harder A, Scheibe B, Wildgruber R, Weiss W (2000) The current state of two-dimensional electrophoresis with immobilized pH gradients. *Electrophoresis* **21**: 1037-1053

Gorg A, Postel W, Gunther S (1988) The current state of two-dimensional electrophoresis with immobilized pH gradients. *Electrophoresis* **9**: 531-546

Görg A, Weiss W, Dunn M (2004) Current two-dimensional electrophoresis technology for proteomics. *Proteomics* **4**: 3665-3685

Habjan M, Penski N, Wagner V, Spiegel M, Overby AK, Kochs G, Huiskonen JT, Weber F (2009) Efficient production of Rift Valley fever virus-like particles: The antiviral protein MxA can inhibit primary transcription of bunyaviruses. *Virology* **385**: 400-408

Handford MG, Carr JP (2007) A defect in carbohydrate metabolism ameliorates symptom severity in virus-infected *Arabidopsis thaliana*. *Journal of General Virology* **88**: 337-341

Hatsugai N, Kuroyanagi M, Yamada K, Meshi T, Tsuda S, Kondo M, Nishimura M, Hara-Nishimura I (2004) A plant vacuolar protease, VPE, mediates virus-induced

hypersensitive cell death. *Science* **305**: 855-858

Hayat S, Ali B, Hasan SA, Ahmad A (2007) Brassinosteroid enhanced the level of antioxidants under cadmium stress in *Brassica juncea*. *Environmental and Experimental Botany* **60**: 33-41

He HQ, Li JX (2008) Proteomic analysis of phosphoproteins regulated by abscisic acid in rice leaves. *Biochemical and Biophysical Research Communications* **371**: 883-888

Hendrickson L, Sharwood R, Ludwig M, Whitney SM, Badger MR, Von Caemmerer S (2007) The effects of Rubisco activase on C-4 photosynthesis and metabolism at high temperature. In *14th International Congress of Photosynthesis*, pp 1789-1798. Glasgow, SCOTLAND

Henzel WJ, Billeci TM, Stults JT, Wong SC, Grimley C, Watanabe C (1993) Identifying proteins from 2-dimensional gels by molecular mass searching of peptide-fragments in protein-sequence databases. *Proceedings of the National Academy of Sciences of the United States of America* **90**: 5011-5015

Higuchi R, Fockler C, Dollinger G, Watson R (1993) Kinetic pcr analysis - real-time monitoring of dna amplification reactions. *Bio-Technology* **11**: 1026-1030

Hofius D, Tsitsigiannis DI, Jones JDG, Mundy J (2007) Inducible cell death in plant immunity. *Seminars in Cancer Biology* **17**: 166-187

Hogle JM, Maeda A, Harrison SC (1986) Structure and assembly of turnip crinkle virus .1. x-ray crystallographic structure-analysis at 3.2 a resolution. *Journal of Molecular Biology* **191**: 625-638

Hollywood K, Brison DR, Goodacre R, Xo (2006) Metabolomics: Current technologies and future trends. *Proteomics* **6**: 4716-4723

Hong F, Lee J, Song JW, Lee SJ, Ahn H, Cho JJ, Ha J, Kim SS (2002) Cyclosporine blocks muscle differentiation by inducing oxidative stress and by inhibiting the peptidylprolyl-cis-trans-isomerase activity of cyclophilin A: cyclophilin A protects myoblasts from cyclosporine-induced cytotoxicity. *Faseb Journal* **16**: 1633-+

Issaq HJ, Veenstra TD (2008) Two-dimensional polyacrylamide gel electrophoresis (2D-PAGE): advances and perspectives. *Biotechniques* **44**: 697-+

Ju HJ, Samuels TD, Wang YS, Blancaflor E, Payton M, Mitra R, Krishnamurthy K,

Nelson RS, Verchot-Lubicz J (2005) The potato virus X TGBp2 movement protein associates with endoplasmic reticulum-derived vesicles during virus infection. *Plant Physiology* **138**: 1877-1895

Julka S, Regnier F (2004) Quantification in proteomics through stable isotope coding: A review. *Journal of Proteome Research* **3**: 350-363

Kabakov AE, Malyutina YV, Latchman DS (2006) Hsf1-mediated stress response can transiently enhance cellular radioresistance. *Radiation Research* **165**: 410-423

Kamoun S, Huitema E, Vleeshouwers V (1999) Resistance to oomycetes: a general role for the hypersensitive response? *Trends in Plant Science* **4**: 196-200

Kaniuga Z (2008) Chilling response of plants: importance of galactolipase, free fatty acids and free radicals. *Plant Biology* **10**: 171-184

Kazan K, Manners JM (2009) Linking development to defense: auxin in plant-pathogen interactions. *Trends in Plant Science* **14**: 373-382

Khurana SMP, Pandey SK, Sarkar D, Chanemougasoundharam A (2005) Apoptosis in plant disease response: A close encounter of the pathogen kind. *Current Science* **88**: 740-752

Kim JL, Morgenstern KA, Griffith JP, Dwyer MD, Thomson JA, Murcko MA, Lin C, Caron PR (1998) Hepatitis C virus NS3 RNA helicase domain with a bound oligonucleotide: the crystal structure provides insights into the mode of unwinding. *Structure* **6**: 89-100

Klose J (1975a) Protein mapping by combined isoelectric focusing and electrophoresis of mouse tissues. A novel approach to testing for induced point mutations in mammals. *Humangenetik* **26**: 231-243

Klose J (1975b) Protein mapping by combined isoelectric focusing and electrophoresis of mouse tissues. A novel approach to testing for induced point mutations in mammals. *Humangenetik* **26**: 231-243

Klose J, Kobalz U (1995) 2-dimensional electrophoresis of proteins - an updated protocol and implications for a functional-analysis of the genome. *Electrophoresis* **16**: 1034-1059

Knopf JA, Shapira M (2005) Degradation of Rubisco SSU during oxidative stress triggers aggregation of Rubisco particles in *Chlamydomonas reinhardtii*. *Planta* **222**:

787-793

Kong QZ, Oh JW, Carpenter CD, Simon AE (1997) The coat protein of turnip crinkle virus is involved in subviral RNA-mediated symptom modulation and accumulation. *Virology* **238**: 478-485

Kovac M, Muller A, Jarh DM, Milavec M, Duchting P, Ravnikar M (2009) Multiple hormone analysis indicates involvement of jasmonate signalling in the early defence of potato to potato virus Y-NTN. *Biologia Plantarum* **53**: 195-199

Kuta DD, Tripathi L (2005) Agrobacterium-induced hypersensitive necrotic reaction in plant cells: a resistance response against Agrobacterium-mediated DNA transfer. *African Journal of Biotechnology* **4**: 752-757

Kwon SJ, Choi EY, Choi YJ, Ahn JH, Park OK, Ky (2006) Proteomics studies of post-translational modifications in plants. *Journal of Experimental Botany* **57**: 1547-1551

Lathem WW, Price PA, Miller VL, Goldman WE (2007) A plasminogen-activating protease specifically controls the development of primary pneumonic plague. *Science* **315**: 509-513

Lawlor DW, Tezara W (2009) Causes of decreased photosynthetic rate and metabolic capacity in water-deficient leaf cells: a critical evaluation of mechanisms and integration of processes. *Annals of Botany* **103**: 561-579

Liang Y, Chen H, Tang MJ, Yang PF, Shen SH (2007) Responses of *Jatropha curcas* seedlings to cold stress: photosynthesis-related proteins and chlorophyll fluorescence characteristics. *Physiologia Plantarum* **131**: 508-517

Lin B, Heaton LA (1999) Mutational analyses of the putative calcium binding site and hinge of the turnip crinkle virus coat protein. *Virology* **259**: 34-42

Livak KJ, Schmittgen TD (2001) Analysis of relative gene expression data using real-time quantitative PCR and the 2(T)(-Delta Delta C) method. *Methods* **25**: 402-408

Loebenstein G (2006) Potato virus diseases, their diagnosis and preparation of virus-tested seed potatoes by rapid propagation. In *3rd Balkan Symposium on Vegetables and Potatoes*, pp 437-439. Bursa, TURKEY

Lu YD, Gan QH, Chi XY, Qin S (2008) Roles of microRNA in plant defense and

virus offense interaction. *Plant Cell Reports* **27**: 1571-1579

Luu-The V, Paquet N, Calvo E, Cumps J (2005) Improved real-time RT-PCR method for high-throughput measurements using second derivative calculation and double correction. *Biotechniques* **38**: 287-293

Majoul T, Bancel E, Triboui E, Ben Hamida J, Branlard G (2003) Proteomic analysis of the effect of heat stress on hexaploid wheat grain: Characterization of heat-responsive proteins from total endosperm. *Proteomics* **3**: 175-183

Marathe R, Guan Z, Anandalakshmi R, Zhao HY, Dinesh-Kumar SP (2004) Study of *Arabidopsis thaliana* resistome in response to cucumber mosaic virus infection using whole genome microarray. *Plant Molecular Biology* **55**: 501-520

Martin GB, Bogdanove AJ, Sessa G (2003) Understanding the functions of plant disease resistance proteins. *Annual Review of Plant Biology* **54**: 23-61

Mauch-Mani B, Mauch F (2005) The role of abscisic acid in plant-pathogen interactions. *Current Opinion in Plant Biology* **8**: 409-414

McLean BG, Zupan J, Zambryski PC (1995) Tobacco mosaic virus movement protein associates with the cytoskeleton in tobacco cells. *Plant Cell* **7**: 2101-2114

Mittler R, Feng XQ, Cohen M (1998) Post-transcriptional suppression of cytosolic ascorbate peroxidase expression during pathogen-induced programmed cell death in tobacco. *Plant Cell* **10**: 461-473

O'Farrell P (1975) High resolution two-dimensional electrophoresis of proteins. *J Biol Chem* **250**: 4007-4021

Ohgawara T, Kobayashi S (1991) Application of protoplast fusion to citrus breeding. *Food Biotechnology* **5**: 169-184

Patton WF (2002) Detection technologies in proteome analysis. *Journal of Chromatography B-Analytical Technologies in the Biomedical and Life Sciences* **771**: 3-31

Peremyslov VV, Hagiwara Y, Dolja VV (1999) HSP70 homolog functions in cell-to-cell movement of a plant virus. *Proceedings of the National Academy of Sciences of the United States of America* **96**: 14771-14776

Persidis A, Ze (1998) Proteomics - An ambitious drug development platform attempts

to link gene sequence to expressed phenotype under various physiological states. *Nature Biotechnology* **16**: 393-394

Piepenbrink MS, Li XH, O'Connell PH, Schat KA (2009) Marek's disease virus phosphorylated polypeptide pp38 alters transcription rates of mitochondrial electron transport and oxidative phosphorylation genes. *Virus Genes* **39**: 102-112

Potter E, Beator J, Kloppstech K (1996) The expression of mRNAs for light-stress proteins in barley: Inverse relationship of mRNA levels of individual genes within the leaf gradient. *Planta* **199**: 314-320

Qu F, Morris TJ (2005) Suppressors of RNA silencing encoded by plant viruses and their role in viral infections. *Febs Letters* **579**: 5958-5964

Qu F, Ren T, Morris TJ (2003) The coat protein of turnip crinkle virus suppresses posttranscriptional gene silencing at an early initiation step. *Journal of Virology* **77**: 511-522

Rathjen JP, Moffett P (2003) Early signal transduction events in specific plant disease resistance. *Current Opinion in Plant Biology* **6**: 300-306

Rathus C, Birch RG (1992) Optimization of conditions for electroporation and transient expression of foreign genes in sugarcane protoplasts. *Plant Science* **81**: 65-74

Ren T, Qu F, Morris TJ (2005) The nuclear localization of the Arabidopsis transcription factor TIP is blocked by its interaction with the coat protein of Turnip crinkle virus. *Virology* **331**: 316-324

Restrepo S, Myers KL, del Pozo O, Martin GB, Hart AL, Buell CR, Fry WE, Smart CD (2005) Gene profiling of a compatible interaction between *Phytophthora infestans* and *Solanum tuberosum* suggests a role for carbonic anhydrase. *Molecular Plant-Microbe Interactions* **18**: 913-922

Robert-Seilaniantz A, Navarro L, Bari R, Jones JD (2007) Pathological hormone imbalances. *Current Opinion in Plant Biology* **10**: 372-379

Rodio ME, Delgado S, De Stradis A, Gomez MD, Flores R, Di Serio F (2007) A viroid RNA with a specific structural motif inhibits chloroplast development. *Plant Cell* **19**: 3610-3626

Romero-Puertas MC, Perazzolli M, Zago ED, Delledonne M (2004) Nitric oxide

- signalling functions in plant-pathogen interactions. *Cellular Microbiology* **6**: 795-803
- Rossignol M, Peltier JB, Mock HP, Matros A, Maldonado AM, Jorin JV (2006) Plant proteome analysis: A 2004-2006 update. *Proteomics* **6**: 5529-5548
- Ryu HS, Song MY, Kim CY, Han MH, Lee SK, Ryoo N, Cho JI, Hahn TR, Jeon JS (2009) Proteomic analysis of rice mutants susceptible to *Magnaporthe oryzae*. *Plant Biotechnology Reports* **3**: 167-174
- Saibo NJM, Lourenco T, Oliveira MM (2009) Transcription factors and regulation of photosynthetic and related metabolism under environmental stresses. *Annals of Botany* **103**: 609-623
- Salvucci ME (2007) Association of Rubisco activase with chaperonin-60 beta: a possible mechanism for protecting photosynthesis during heat stress. In *14th International Congress of Photosynthesis*, pp 1923-1933. Glasgow, SCOTLAND
- Salvucci ME, Crafts-Brandner SJ (2004) Inhibition of photosynthesis by heat stress: the activation state of Rubisco as a limiting factor in photosynthesis. *Physiologia Plantarum* **120**: 179-186
- Salvucci ME, Osteryoung KW, Crafts-Brandner SJ, Vierling E (2001) Exceptional sensitivity of rubisco activase to thermal denaturation in vitro and in vivo. *Plant Physiology* **127**: 1053-1064
- Salvucci ME, Werneke JM, Ogren WL, Portis AR (1987) Purification and species distribution of rubisco activase. *Plant Physiology* **84**: 930-936
- Sampol B, Bota J, Riera D, Medrano H, Flexas J (2003) Analysis of the virus-induced inhibition of photosynthesis in malmsey grapevines. *New Phytologist* **160**: 403-412
- Santoro MG (1994) Heat-shock proteins and virus-replication - hsp70s as mediators of the antiviral effects of prostaglandins. *Experientia* **50**: 1039-1047
- Saravanan RS, Rose JKC (2004) A critical evaluation of sample extraction techniques for enhanced proteomic analysis of recalcitrant plant tissues. *Proteomics* **4**: 2522-2532
- Sharma D, Masison DC (2009) Hsp70 Structure, Function, Regulation and Influence on Yeast Prions. *Protein and Peptide Letters* **16**: 571-581
- Shigeoka S, Ishikawa T, Tamoi M, Miyagawa Y, Takeda T, Yabuta Y, Yoshimura K

(2001) Regulation and function of ascorbate peroxidase isoenzymes. In *Annual Meeting of the Society-for-Experimental-Biology*, pp 1305-1319. Canterbury, England

Shih WL, Liao MH, Yu FL, Lin PY, Hsu HY, Chiu SJ (2008) AMF/PGI transactivates the MMP-3 gene through the activation of Src-RhoA-phosphatidylinositol 3-kinase signaling to induce hepatoma cell migration. *Cancer Letters* **270**: 202-217

Siddiqui MH, Khan MN, Mohammad F, Khan MMA (2008) Role of nitrogen and gibberellin (GA(3)) in the regulation of enzyme activities and in osmoprotectant accumulation in *Brassica juncea* L. under salt stress. *Journal of Agronomy and Crop Science* **194**: 214-224

Slaymaker DH, Navarre DA, Clark D, del Pozo O, Martin GB, Klessig DF (2002) The tobacco salicylic acid-binding protein 3 (SABP3) is the chloroplast carbonic anhydrase, which exhibits antioxidant activity and plays a role in the hypersensitive defense response. *Proceedings of the National Academy of Sciences of the United States of America* **99**: 11640-11645

Song XS, Wang YJ, Mao WH, Shi K, Zhou YH, Nogue S, Yu JQ (2009) Effects of cucumber mosaic virus infection on electron transport and antioxidant system in chloroplasts and mitochondria of cucumber and tomato leaves. *Physiologia Plantarum* **135**: 246-257

Subramaniam R, Desveaux D, Spickler C, Michnick SW, Brisson N (2001) Direct visualization of protein interactions in plant cells. *Nature Biotechnology* **19**: 769-772

Sun XP, Zhang GH, Simon AE (2005) Short internal sequences involved in replication and virion accumulation in a subviral RNA of Turnip crinkle virus. *Journal of Virology* **79**: 512-524

Tang X, Rolfe SA, Scholes JD (1996) The effect of *Albugo candida* (white blister rust) on the photosynthetic and carbohydrate metabolism of leaves of *Arabidopsis thaliana*. *Plant Cell and Environment* **19**: 967-975

Teulier C, Grimapettenati J, Curie C, Teissie J, Boudet AM (1991) Transient foreign gene-expression in polyethylene-glycol treated or electropulsated eucalyptus-gunnii protoplasts. *Plant Cell Tissue and Organ Culture* **25**: 125-132

Thomas CL, Leh V, Lederer C, Maule AJ (2003) Turnip crinkle virus coat protein mediates suppression of RNA silencing in *Nicotiana benthamiana*. *Virology* **306**: 33-41

- Timperio AM, Egidi MG, Zolla L (2008) Proteomics applied on plant abiotic stresses: Role of heat shock proteins (HSP). *Journal of Proteomics* **71**: 391-411
- Tognetti VB, Zurbriggen MD, Morandi EN, Fillat MF, Valle EM, Hajirezaei MR, Carrillo N (2007) Enhanced plant tolerance to iron starvation by functional substitution of chloroplast ferredoxin with a bacterial flavodoxin. *Proceedings of the National Academy of Sciences of the United States of America* **104**: 11495-11500
- Vasudevan A, Oh TK, Park JS, Lakshmi SV, Choi BK, Kim SH, Lee HJ, Ji J, Kim JH, Ganapathi A, Kim SC, Choi CW (2008) Characterization of resistance mechanism in transgenic *Nicotiana benthamiana* containing Turnip crinkle virus coat protein. *Plant Cell Reports* **27**: 1731-1740
- Wang B, Li FH, Dong B, Zhang XJ, Zhang CS, Xiang JH (2006) Discovery of the genes in response to white spot syndrome virus (WSSV) infection in *Fenneropenaeus chinensis* through cDNA microarray. *Marine Biotechnology* **8**: 491-500
- Wang HL, Hao LM, Wen JQ, Zhang CL, Liang HG (1998) Differential expression of photosynthesis-related genes of reed ecotypes in response to drought and saline habitats. *Photosynthetica* **35**: 61-69
- Wendehenne D, Durner J, Chen ZX, Klessig DF (1998) Benzothiadiazole, an inducer of plant defenses, inhibits catalase and ascorbate peroxidase. *Phytochemistry* **47**: 651-657
- Yan SP, Zhang QY, Tang ZC, Su WA, Sun WN (2006) Comparative proteomic analysis provides new insights into chilling stress responses in rice. *Molecular & Cellular Proteomics* **5**: 484-496
- Yoo TH, Park CJ, Lee GJ, Shin R, Yun JH, Kim KJ, Rhee KH, Paek KH (2002) A hot pepper cDNA encoding ascorbate peroxidase is induced during the incompatible interaction with virus and bacteria. *Molecules and Cells* **14**: 75-84
- Zhang DH, Tai LK, Wong LL, Chiu LL, Sethi SK, Koay ESC (2005) Proteomic study reveals that proteins involved in metabolic and detoxification pathways are highly expressed in HER-2/neu-positive breast cancer. *Molecular & Cellular Proteomics* **4**: 1686-1696
- Zhao YJ, DelGrosso L, Yigit E, Dempsey DA, Klessig DF, Wobbe KK (2000) The amino terminus of the coat protein of Turnip crinkle virus is the AVR factor recognized by resistant *Arabidopsis*. *Molecular Plant-Microbe Interactions* **13**: 1015-1018

Zhao ZY, Yin ZX, Weng SP, Guan HJ, Li SD, Xing K, Chan SM, He JG (2007) Profiling of differentially expressed genes in hepatopancreas of white spot syndrome virus-resistant shrimp (*Litopenaeus vannamei*) by suppression subtractive hybridisation. *Fish & Shellfish Immunology* **22**: 520-534

Zhou SM, Liu WN, Kong LA, Wang M (2008) Systemic PCD occurs in TMV-tomato interaction. *Science in China Series C-Life Sciences* **51**: 1009-1019